Reconstructing sea surface salinity variability from Porites corals in the Indonesian Berau delta system

By
Henk Lenderink
3699897

Utrecht University, MSc thesis
Earth, Life and Climate

June 2016

Supervised by:
Prof. Gert-Jan Reichart
Dr. Rick Hennekam

Abstract

Sea surface salinity is a crucial parameter for global ocean circulation and climate reconstruction. However, until now there is a lack of proxies that can be directly related to salinity. Na/Ca in foraminiferal carbonate is potentially such a proxy (Wit et al., 2013), which has never been applied to coral carbonate. Corals are known to be excellent recorders of environmental variability with strong age control with sub-seasonal resolution. This study explores the potential of the Na/Ca proxy from coral carbonate. A transect with a strong salinity gradient through the Berau delta is used as a natural laboratory to test several conventional sea surface salinity proxies (seawater $\delta^{18}O$, Ba/Ca, G/B ratio) and the Na/Ca proxy from *Porites* coral carbonate. The data of the Na/Ca proxy showed clear seasonal cycles corresponding to the expected salinity fluctuations due to changes in river runoff. However, no correlation was found between the Na/Ca proxy and the other conventional runoff and salinity proxies, nor the climate indices. The conventional proxies were also used to assess the most important climatological drivers in eastern Kalimantan up to 1970. The most important climatologic factor influencing the Berau delta system seems to be the El Niño-Southern Oscillation. This climatic variability has a large impact on the precipitation over the Berau catchment area, and thus the amount of runoff by the Berau River. Changes in the precipitation over the area do not necessarily lead to an increase in erosion and sediment supply for the Berau River, although the decrease in forest cover in the catchment area, in combination with the increase in precipitation will potentially lead to an increase in sediment supply for the Berau delta. This will have a major effect on the corals that are located close to the Berau delta shoreline.

Universiteit Utrecht

NIOZ

Table of contents

1. Introduction

Anthropogenic climate change is one of the most important issues threatening the planet in the present time. A major component driving climate variability is ocean circulation. Salinity, in conjunction with temperature, controls ocean water density, which largely drives the hydrological cycle in the ocean basins (Bindoff et al., 2013). Hence, it is a vital environmental parameter, which also affects stratification and thereby the capacity to store organic carbon and heat in the ocean at depth (Rhein et al., 2013). Moreover, surface ocean salinity can be used as a proxy for precipitation and evaporation over the ocean (Cahyarini et al., 2008; Zinke et al., 2005; Grove et al., 2013; Rhein et al., 2013; Moreau et al., 2015). Hence, salinity is a key component to gather information about climate variability and its change.

Past salinity reconstructions heavily rely on (geochemical) proxies (Henderson, 2002), as instrumental records with salinity data are relatively short term (generally max. 150 years). Corals are one of the most suitable archives of salinity (and temperature) due to their high resolution carbonate sequences, strong chronological control, and their high sensitivity to register environmental variability. One of the most suitable coral for reconstructing past ocean parameters is the *Porites* genus due to the fact that they are widely distributed in the Pacific and Indian Oceans, strongly resistant to erosion, and grow very large in size (Moreau et al., 2015).

Nowadays different proxies, such as $\delta^{18}O$, $\delta^{13}C$, Ba/Ca, and Green/Blue (G/B) spectral luminescence ratios from UV light, are influenced by - and therefore used to - reconstruct freshwater inflow and related surface seawater salinity from massive *Porites* communities (Corrège, 2006; Cahyarini et al., 2008; Grove et al., 2010; Moreau et al., 2015). Sr/Ca and Mg/Ca ratios are commonly used as sea surface temperature proxies, although Mg/Ca is also influenced by other oceanic variabilities such as salinity (Rohling, 2000; Henderson, 2002; Moreau et al., 2015). Sr/Ca ratio can be used as temperature proxy to correct coral $\delta^{18}O$ for the temperature effect, so that the remaining seawater $\delta^{18}O$ ($\delta^{18}O_{sw}$) variability reflects changes in salinity (Ren et al., 2003). The Ba/Ca ratio, as well as the Green/Blue (G/B) ratio obtained during line-scanning under UV light, can be used as a proxy for river outflow (Sinclair and McCulloch, 2004; Grove et al., 2010). However, none of the existing proxies for river runoff and associated salinity are direct derivatives from ocean water salt, while a direct proxy would possibly result in better reconstructions of salinity. Na/Ca from coral carbonates could potentially provide such a direct reflection of salinity, similar to Na/Ca from foraminiferal carbonate, which is already used (Wit et al., 2013). This MSc thesis will analyse Na/Ca ratio as a new salinity proxy from coral carbonates and use the other described proxies to make a robust reconstruction of the climatic variability of the research area (i.e. Berau delta region) extending the existing instrumental record.

Specifically, the objective of this MSc thesis is to reconstruct the climate variability of the Southeast Asia region over the last few decades, aiming at the coral sampled from the Indonesian Berau delta system. Different coral slabs in a transect from the river mouth of the Berau River to the open ocean were used for this reconstruction. One of the slabs, with a long record and clear visible annual banding, was used for the development of the potential Na/Ca salinity proxy by using different techniques (Laser Ablation ICP-MS linescan and line of spots and Sector Field ICP-MS).

The results of the Na/Ca measurements will be compared with other potential salinity proxies, such as $\delta^{18}O_{sw}$, Ba/Ca and G/B ratios, to validate the Na/Ca proxy. Ultimately, together with the other proxy datasets ($\delta^{18}O$, $\delta^{13}C$, Sr/Ca, Mg/Ca), this will give a good estimation of the climatic variability that took place in the Berau delta, while it will also be a thorough test of the Na/Ca as a potential salinity proxy in corals.

2. Background

2.1. Regional settings

2.1.1. Berau delta/barrier reef system

The Berau delta/barrier reef system is located at the East coast of Kalimantan, Indonesia (Figure 1). The system is part of the Coral Triangle and is distinguished by its high coral diversity. The Berau system is influenced by both fluvial and oceanic factors: the Berau River in the west and the Indonesian Throughflow (ITF) that flows from the north to the south through the adjacent Makassar Strait. The Berau River is responsible for fresh water and sediment input into the Delta system. The ITF on the other hand is a critical point in the global ocean circulation, transporting heat and salt from the Pacific to the Indian Ocean.

The Berau delta system is presumably influenced by different climatic events, most likely the most important ones are monsoon events, the El Niño-Southern Oscillation (ENSO), Pacific Decadal Oscillation (PDO), and the Indian Ocean Dipole (IOD) [see *2.3. climatic settings*] (Saji et al., 1999; Trenberth et al., 2007; KNAW, 2016). Besides these seasonal (i.e. monsoon) and interannual (i.e. ENSO, PDO, and IOD) climate variability, also the tidal fluctuations have an important effect on the area, as they contribute to the shaping of the Delta. The tidal range for the Berau delta varies between 1 and 2.5 meter (Buschman et al., 2012).

A 40 kilometres long coral reef area is located at the shelf break, 40 kilometres (north)-east of the Berau River mouth (Figure 1). The water depth east of the reef rapidly increases up to 3000 m in a deep trench of the Makassar Strait (Tarya et al., 2015).

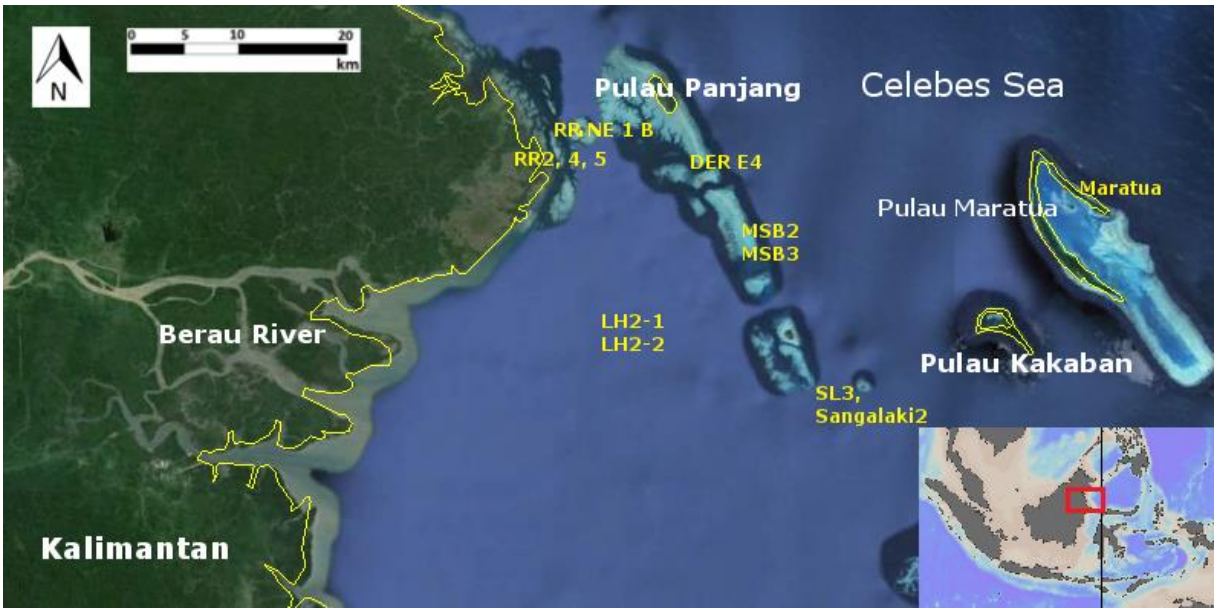

Figure 1. Map of the Berau delta system at the coast of East Kalimantan. In yellow the position of the 12 coral samples used for this research.

2.1.2. The Berau River

With a total catchment of about 14.000 square kilometres, the Berau River combines the Kayan and Mahakam rivers (Buschman et al., 2012). The catchment area of the Berau River mainly consists of a mountainous rainforest, although the forest is decreasing rapidly due to commercial logging for oil

palm (see Table 1), most likely leading to an increase in soil erosion and sediment fluxes. The discharge of the river fluctuates between 135 and 1412 $m^3 s^{-1}$, with an average of 605 $m^3 s^{-1}$ (Buschman et al., 2009). Buschman et al (2012) observed a 2 Mt y^{-1} flux of suspended sediment as the upper limit of yearly averaged sediment flux. These fluxes can increase in the near future by 10-100 times due to land cover changes (Buschman et al., 2012). Precipitation is the most important factor that contributes to the discharge and the sediment flux of the Berau River. Measurements at the Meteorological and Geophysical Agency (Badan Meteorologi dan Geofisika - BMG) station in Tanjung Redeb (East Kalimantan – 2.15°N 117.47°E) between 1987 and 2007 show the highest average precipitation in the boreal winter months, where temperature only varies slightly in this area (Figure 2). The linear trend of the data shows an increase in both temperature and precipitation in modern times. Precipitation increases every year with approximately 3mm and temperature increases with 1 degree every 16 years.

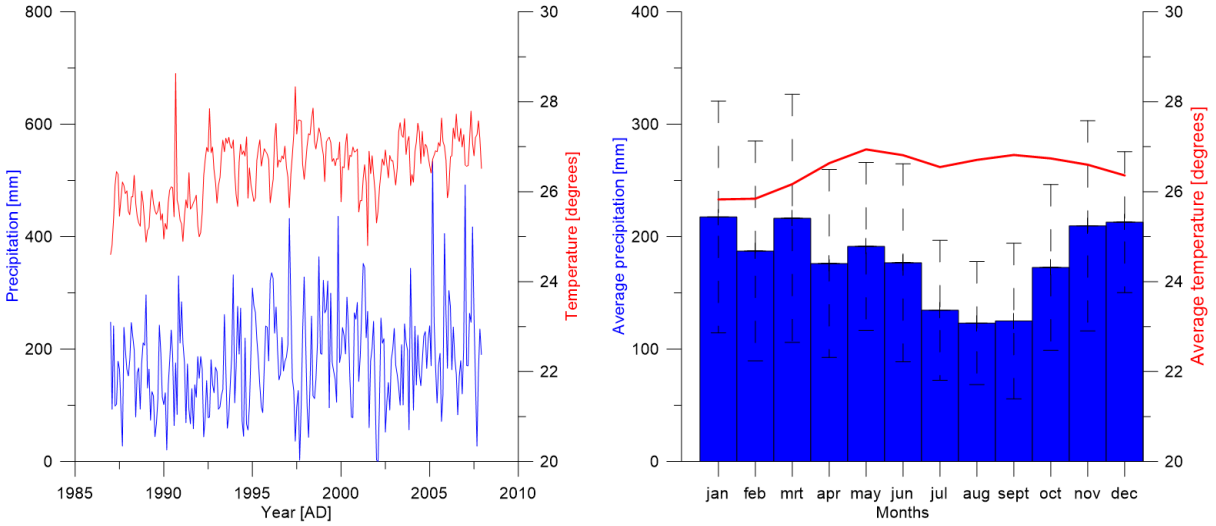

Figure 2. Left: precipitation (blue) and temperature (red) data of the Meteorological and Geophysical Agency (Badan Meteorologi dan Geofisika - BMG) in Tanjung Redeb. Right: average monthly precipitation (blue) and temperature (red) data. Error bars for the monthly precipitation show the standard deviation of the data.

	1995	2000	2005	2008
Undisturbed	12 196	8407	7551	4319
Logged-over	7121	7991	9497	5766
Total	19 317	16 398	17 048	10 085

Table 1. Forest cover (km^2) in the Berau catchment area over time after Buschman et al. (2012).

Besides the amount of runoff and sediment flux, also the river plume of the Berau River shows an annual cyclicity. Tarya et al. (2015) used observation data incorporated in a three-dimensional model (ECOMSED) to reconstruct this river plume (see Figure 3). Due to shifts in wind direction, the river plume of the Berau River is directed towards the coral reef between the months march and august. During the other months the river plume is directed to the south, so that the coral reef will have less impact of the Berau River in these months.

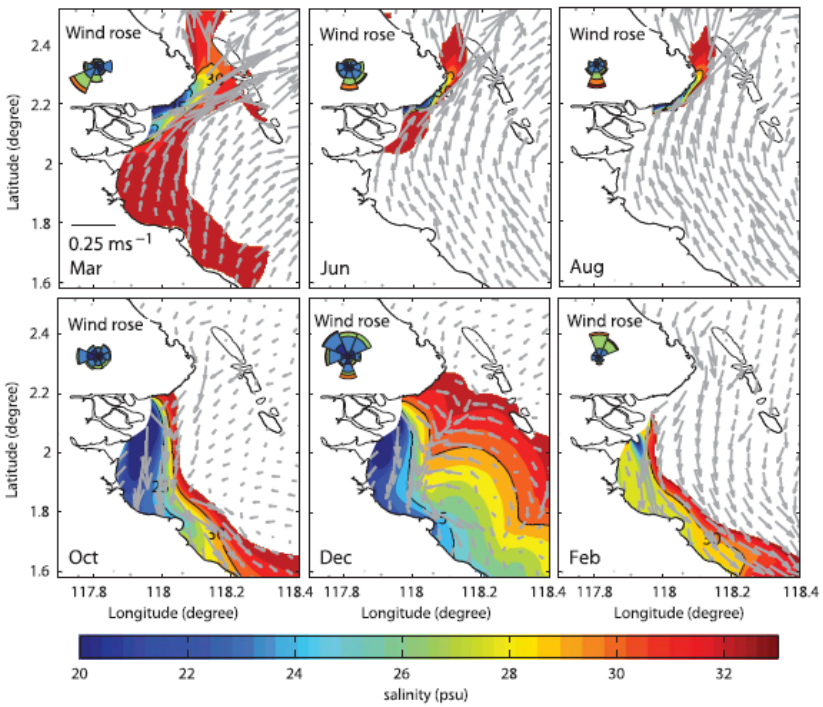

Figure 3. Changes in river plume of the Berau River, modified after Tarya et al. (2015). The different colours indicate the modelled salinity in psu.

Due to the combination of precipitation data and the fluctuations in river plume, the peak in impact of the Berau River for the coral occurs around March. March shows high precipitation for the research area and the southwest orientated wind direction pushes the river plume to the north coast of the Berau delta; the location where most of the coral is situated.

2.2. Oceanographic setting

2.2.1. Indonesian Throughflow

The Indonesian Throughflow (ITF) is an important part of the global ocean circulation, as it transports relatively warm and lower saline waters from the western Pacific towards the Indian Ocean. With about 80% of the total throughflow, the primary path of the ITF is through the narrow Makassar Strait between Borneo and Sulawesi (Figure 4) (Tillinger and Gordon, 2009). The fluctuation of the ITF is highly related to El Niño-Southern Oscillation (ENSO) and Asian monsoon events, although the exact correlation between these climatic events and the ITF is still highly debated (Tillinger and Gordon, 2009; van Sebille et al., 2014). During the northwest monsoon, eastward zonal winds shift low saline, buoyant waters from the Java Sea and the South China Sea to the southern Makassar Strait. This leads to a decrease in pressure gradient between the Pacific and the Indian Ocean, causing the blocking of ITF surface transport through the Makassar Strait (Gordon et al., 2003). During the southeast monsoon this process is reversed and the ITF is enhanced (Wyrtki, 1987).

During a La Niña event, strong easterlies build up a high sea level in the western Pacific, leading to a higher pressure difference between the western Pacific and the Indian Ocean (Meyers, 1996). This increased pressure difference results in an increase in the ITF. This mechanism is reversed during an El Niño event (Grove, 2012, Liu et al., 2015).

The ITF is highly responsible for the regulation of precipitation in Indonesia, India and Australia (Ambarwulan, 2010). The ITF can be estimated by using interocean pressure differences between the Pacific and the Indian Ocean (Tillinger & Gordon, 2009) [see *3.8. Indonesian Throughflow*].

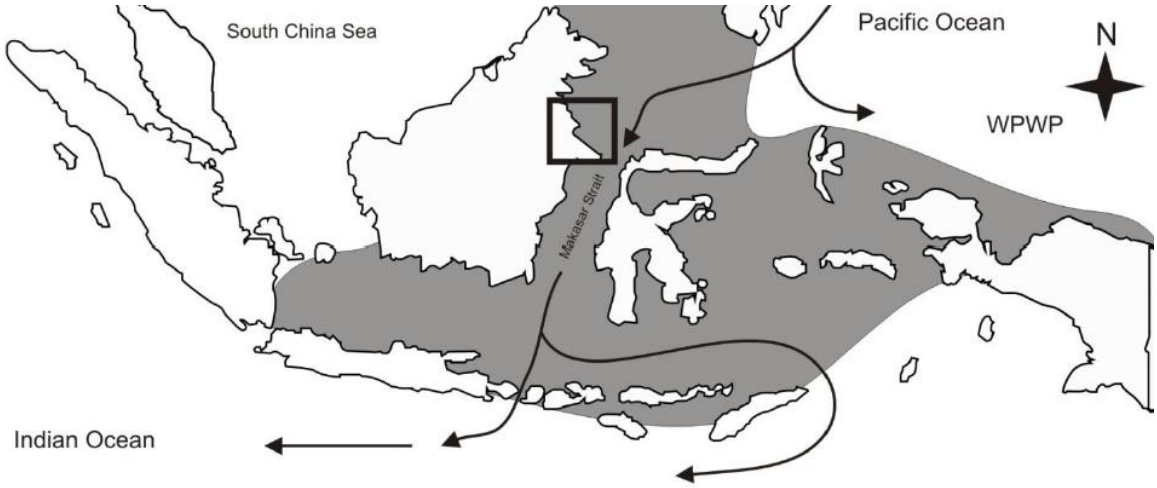

Figure 4: Pathway of the ITF, transporting warm low saline water from the Pacific Ocean to the Indian Ocean. The main pathway is through the Makassar Strait, indicated by the black arrows. The research area is located in the black box. Figure modified after Pascher (2012).

2.3. Climatic setting

2.3.1. Monsoons

The Berau delta system is influenced by two monsoon seasons through the year: A warm and dry southeast monsoon from May to September and a warm and wet northwest monsoon from November to March (Wyrtki, 1987). The Intertropical Convergence Zone (ITCZ) represents the maximum solar heating at a given time and latitude, leading to a belt of high cloud cover and precipitation in the area where the northeast and southeast trade winds converge. During boreal summer, the ITCZ is located above the Asian Continent. Due to strong warming, a low pressure system is formed above the mainland of Asia and a high pressure system is established above the ocean (Wyrtki, 1987). This leads to the movement of moist air to land, leading to high precipitation above India, known as the northern hemisphere summer monsoon (southeast monsoon). Synchronously, the southeast trade winds carry dry air from Australia towards the north, resulting in low precipitation in the Berau system at that time. During the northwest monsoon, the low pressure ITCZ is settled directly above the Berau system, leading to the movement of moist air from the Indian and Pacific Ocean to the Berau delta, causing a higher precipitation rate in the research area (Wyrtki, 1987).

2.3.2. El Niño-Southern Oscillation

The El Niño-Southern Oscillation (ENSO) is a quasiperiodic atmosphere-ocean event that has large impact on the Berau system (Ropelewski & Halpert, 1987). El Niño refers to the phase that is characterized by warming of Pacific surface waters near the equator at the west coast of South America, weakening the gradient of sea surface temperature (SST) between the east and west side of the Pacific. El Niño events occur every 3 to 7 years in alternation with its opposite phase (i.e. La Niña), which is associated with below-average temperatures of the Pacific surface waters near the equator at the west coast of South America (Trenberth et al., 2007). El Niño is closely related to the Southern

Oscillation, which is its atmospheric equivalent. The Southern Oscillation affects changes in precipitation, trade winds and tropical circulation.

Under normal conditions, the cold surface waters from the eastern Pacific are transported to the western Pacific due to equatorial trade winds. These waters are slowly heated, resulting in higher SST in western Pacific water in respect to the eastern Pacific. The positive feedback loop between the strong easterly trade winds and the strong difference in sea surface temperature between the eastern and western part of the Pacific Ocean is known as the Bjerknes feedback (Palmer and Mansfield, 1984) and causes relative warm and wet conditions for the Berau delta area. During an El Niño event, the eastern part of the Pacific Ocean becomes warmer due to a deepening of the thermocline. SST differences between eastern and western Pacific Ocean are decreased as well as the easterly trade winds, resulting in a decrease in precipitation over the Berau delta area. During a La Niña event, the normal conditions with a strong difference in SST between the eastern and western Pacific are enhanced, resulting in an increase in precipitation over the Berau delta area. There are different indices of time series for the ENSO that measure SST anomalies for a certain area in the Pacific Ocean [see *3.8.1. El Niño-Southern Oscillation*].

2.3.3. Indian Ocean Dipole

Similar to the Pacific and Atlantic Ocean, the Indian Ocean has an interannual climate variability as well, known as the Indian Ocean Dipole (IOD) (Saji et al., 1999). Because of the location of the Berau delta system at the gateway between the Pacific and Indian Ocean, the IOD potentially also affects the research area. The IOD is an ocean-atmospheric interaction that causes an alternation of SST in the Indian Ocean (Saji et al., 1999). During a positive IOD event, enhanced eastward equatorial jet streams pushes warm surface water towards the eastern Indian Ocean resulting in strong upwelling of cold water at the western Indian Ocean (Saji et al., 1999). During a negative IOD event, the eastward jet streams are reduced. A positive IOD potentially results in colder and drier conditions for the catchment area of the Berau River. A negative IOD is characterized by higher SST and higher precipitation over Indonesia. The difference in SST between the western and eastern Indian Ocean can be used as an index for the IOD [see *3.8.4. Indian Ocean Dipole*].

2.3.4. Pacific Decadal Oscillation

The Pacific Decadal Oscillation (PDO) is a climate variability caused by changes in atmospheric circulation, SST and ocean circulation in the Pacific, varying on decadal time scales (Mantua et al., 1997). Although it originates at the northern Pacific, research showed a great impact of the PDO in the southern hemisphere pacific (Mantua and Hare, 2002). During a positive PDO, the north-western Pacific contains cold surface waters compared to the eastern part of the Pacific, the opposite pattern occur during a negative index (Mantua and Hare, 2002). Although the effect of the PDO on Indonesia is highly uncertain, the location of the Berau delta system at the throughflow of the Pacific Ocean to the Indian Ocean indicates a possible impact of the PDO on the research area. The PDO shows a good correlation with the ENSO and ITF indices (Wang et al., 2014) [see *3.8.7. Correlation of the different climate indices]*.

2.4. Coral records and climate proxies

2.4.1. Coral records

The Berau delta is part of the Coral Triangle, which covers 5.7 million square kilometre of tropical marine waters in Southeast Asia that cover a high diversity of reef-building corals. Although there are over 500 types of reef-building corals in the area, the most common type is the *Porites* spp. (Renema, 2006) (Figure 5). The Poritadae *Porites* spp. used in this study belong to the scleractinian corals, also known as stony corals. Due to changes in environmental factors such as sun hours, light transparency, nutrient exposure, partial pressures and temperature, the accretion of calcium carbonate varies, which results in banding of the coral structure (Grove, 2012). Generally, the growth rate of *Porites* spp. ranges between 5 and 20 mm per year containing a high and a low density band (Grove, 2012). The carbonate skeleton of the coral can create enormous dome-shaped structures of several meters, which can contain climate and environmental archives of several centuries.

Figure 5. Drilling of the Porites spp. in 2008, photograph by Roel Nagtegaal (After Pascher, 2012).

2.4.2. Coral proxies

The climatic environment is recorded in corals, as they build their calcium carbonate skeletons using the surrounding seawater. Besides the isotopic composition of oxygen and carbon, also trace elements (i.e. Sr, Mg, Al, Ba, Na…) are incorporated in the coral and may reflect the oceanic conditions. This information that is stored in the coral can in most circumstances be used as a proxy indicating conditions such as SST, river outflow, and salinity.

G/B ratio: The Green to Blue ratio (G/B ratio) is a reflection of the humic acid (Green) concentrations in the seawater relative to the amount of aragonite (Blue) of the coral (Grove et al., 2010). Humic acid is derived from terrestrial soils and can therefore be used as a proxy for river runoff of the Berau River (Grove et al., 2015). Generally the G/B ratio is used instead of green intensities alone, to normalize the humic acid signal to the aragonite signal in coral carbonate (Grove et al., 2010). The G/B ratio does not necessarily record the amount of river runoff, because the G/B ratio is also affected by the distance between the river and the coral, the direction of the current and the depth of the coral. For the Berau system, the direction of the current is expected to be very important due to the shift in river plume during a year.

Seawater $\delta^{18}O$: The stable isotope $\delta^{18}O$ ratio of coral skeleton is both a function of SST and the isotopic composition of the sea water itself (Corrège, 2006). The seawater $\delta^{18}O$ ($\delta^{18}O_{sw}$), in turn, often relates to sea surface salinity (SSS) as fresher water has generally a lighter isotopic composition (Fairbanks et

al., 1997). The SST component of the $\delta^{18}O$ ratio can be removed if another proxy is used as a SST measurement [see *3.5. Seawater $\delta^{18}O$ reconstruction*], resulting in a $\delta^{18}O_{sw}$. Although the $\delta^{18}O_{sw}$ can be used as an indirect proxy for salinity, there is no one-to-one relationship between $\delta^{18}O_{sw}$ and salinity due to the shifts of isotopic composition of precipitation and river water (Benway and Mix, 2004).

$\delta^{13}C$: The use of the carbon isotopic ratios ($\delta^{13}C$) in coral skeletons is relatively difficult compared to the $\delta^{18}O$ ratio due to the multiple environmental and physiological factors that affect the signal of the ratio (Watanabe et al., 2002). In recent history, changes in $\delta^{13}C$ ratio were interpreted to be influenced by: 1) inorganic carbon in seawater (Swart et al., 1996); 2) changes in photosynthesis (Swart et al., 1996); 3) skeletal growth rate (de Villiers et al., 1995); 4) bleaching events (Suzuki et al., 2005); and 5) zooplankton abundance (Felis et al., 1998). We will compare the coral $\delta^{13}C$ to other proxies of salinity, as dissolved inorganic carbon of river fresh water has often a relatively light $\delta^{13}C$ value due to the remineralization of terrestrial organic matter (i.e. mainly vegetation) (Swart et al., 1996). Hence, we will test if this signal is observable in our $\delta^{13}C$ data, despite being difficult to interpret due to the influence of many different factors.

Trace elements: Trace elements of coral carbonate are also used to reconstruct climatic variability. The Ba/Ca ratio is often used as a proxy for river outflow as Barium is released from fine-grained suspended clay particles in rivers, and subsequently incorporated in coral carbonate (Sinclair and McCulloch, 2004). Sr/Ca is widely used as a proxy for SST (Marshall and McCulloch, 2002; Cahyarini et al., 2008; Moreau et al., 2015). Another SST proxy often used is the Mg/Ca ratio (Mitsuguchi et al., 1996; Fallon et al., 1999), although it may be less reliably than the Sr/Ca ratio as it may be sensitive for the influence of biological activity and metabolism (Mitsuguchi et al., 2003). Moreau et al. (2015) suggested that besides SST also sea surface salinity (SSS) can affect the Mg/Ca ratio. Although Al/Ca ratio is not widely used as a proxy for coral cores, it is often used as a proxy for contamination at foraminiferal measurements (Barker et al., 2003; Ferguson et al., 2008).

With an average of 15-24 mmol/mol, Na has the highest molar ratio to calcium of all minor elements in coral skeletal aragonite (Ramos et al., 2004; Mitsuguchi et al., 2010). Still, the number of studies about Na/Ca ratio on coral cores is very low. Although clear annual cycles have been found in this ratio (Mitsuguchi et al., 2010), there is almost no discussion about the factors that control the fluctuations in Na/Ca ratio. Mitsuguchi et al. (2010) suggested that Na/Ca is mostly influenced by temperature and salinity, but that also other factors can have an impact on the ratio. This thesis will further look in to the variability in Na/Ca, as in foraminifer carbonate it can be used as a salinity proxy (Wit et al, 2013).

3. Material and methods

3.1. Coral material and treatment

A total of 24 *Porites* spp. Cores were drilled during field campaigns in October 2003, September 2006, May 2007 and August 2008. Drilling was done with a hand-held pneumatic air tool (CRAFTOMAT) with 6 bar working pressure, provided with a 4 cm diameter diamond drill (DIA-G). 12 of the cores could be used for age modelling with their G/B ratio. The properties of these 12 cores are given in Table 2 and positions of these cores can be found in Figure 1.

The cores were prepared for analyses, as described in Pascher (2012). In short, the coral cores where bleached in hydrogen peroxide and rinsed with tap water to remove coarse material such as sea salt. Subsequently, they were cut in 7 mm thick slices with a precision rock saw and cleaned with tap water. The slices were later rinsed 10 minutes in an ultrasonic bath with 17 MΩ ultrapure water for three times (Figure 6a). Loose particles were removed with a compressed filtered air (Figure 6b) before they were dried for 24 hours in a laminar flow hood (Figure 6c). After this, the slices were bleached with reagent grade sodium hypochlorite (NaOCl 10-15% available chlorine Sigma-Aldrich Company) diluted 1:1 with 17MΩ ultrapure water for 24 hours (Figure 6d). The slices were washed with tap water and rinsed twice in a 17MΩ ultrapure water ultrasonic both for 5 minutes. Finally the coral slabs were dried for 24 hours in a laminar flow hood.

Station	Longitude E	Latitude N	Depth top colony [m]	Core length [m]	Date of collection	$\delta^{18}O$ data
RR2	118° 06.46617'	2°19.16577'	2	0.32	Oct. 2003	✓
RR4	118° 06.52571'	2° 19.23948'	3	0.28	Oct. 2003	✓
RR5	118° 06.52571'	2° 19.23948'	3	0.32	Oct. 2003	
RR NE 1B	118°8.22162'	2°20.20862'	-	0.27	Oct. 2003	
Sangalaki2	118°24.31037'	2°5.38834'	-	0.39	Aug. 2008	✓
SL3	118°24.31037'	2°5.38834'	4	0.35	Oct. 2003	
MSB2	118°16.96927'	2°15.40349'	2.1	0.21	Oct. 2003	
MSB3	118°16.96927'	2°15.40349'	4.3	0.25	Oct. 2003	✓
DER-E4	118°15.71152'	2°17.64101'	6	0.16	Oct. 2003	
Maratua	118°37.212'	2°15.991'	-	0.83	May 2007	✓
LH2-1	118°10.187'	2°9.574'	5.5	0.86	Sept. 2006	✓
LH2-2	118°10.187'	2°9.574'	5.5	1.47	Sept. 2006	

Table 2. Coral cores used for this Research. Sampling sites are shown in Figure 1.

Figure 6. Coral cores treatment with: A) Coral slabs rinsed in an ultrasonic bath. B) Cleaning of the coral slab with compressed air. C) Coral slabs dried under a laminar flow hood. D) Bleaching of the coral slabs. Photographs modified after Pascher (2012).

3.2. Spectral luminescence scanning

Spectral luminescence scanning of the coral cores were performed using an Avaatech XRF core-scanner at the NIOZ research institute (Texel, Netherlands) to observe the luminescence bands of the coral slabs (after Grove et al., 2010). A high resolution line-scan camera (71 µm pixel size) with a beam-splitter was used to separate the intensity of the luminescence emissions of the coral carbonate under the UV light into three wavelengths: Red, Green and Blue (RGB) (Figure 7a). To obtain the Green to Blue (G/B) ratio, a 1.5mm wide transect parallel to the growth direction of the coral was measured with Line Scan Software Version 2.0 (Avaatech). In order to reduce the noise, a 0.5mm average of the data was used. In order to avoid the disturbing effects of contamination of the coral, more than one transect was used for most of the coral cores (Figure 7b).

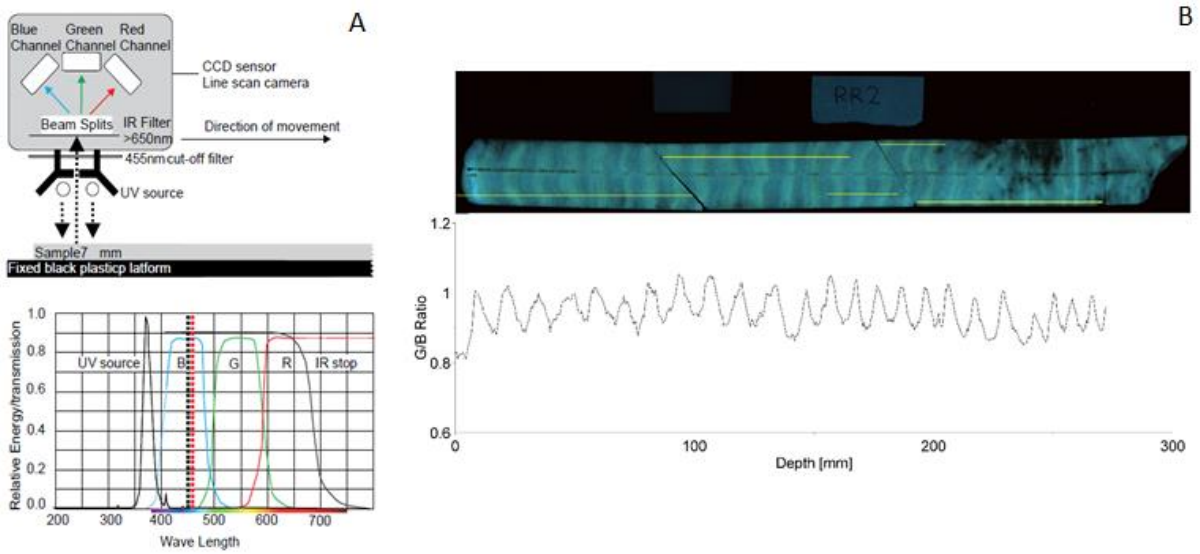

Figure 7. Spectral luminescence scanning: A) Schematic diagram of the modified Avaatch core scanner (derived after Grove et al. (2010)). B) Transect (yellow line) for the RR2 coral slab SLS with the resulting G/B Ratio of the 0.5mm average data.

3.3. Stable isotope and trace element coral preparation

Stable isotope measurements were done for coral slab RR4 (Figure 1). 5 other coral slabs (Table 2) were already measured for stable isotopes ($\delta^{18}O$ and $\delta^{13}C$) and different trace elements (Sr, Ba, Al, Mg and Ca, but no Na) by Pascher (2012). The RR4 core was drilled parallel to major growth axis with a diamond drill (Horico H001 009, 0.9mm diameter, 8.5 volt). Samples were taken every 1.5 mm and were stored in plastic vials. This sampling resolution corresponds to a monthly to bi-monthly resolution of the samples. The coral and drill were cleaned with Milli-Q and compressed air after each drill. A total of 174 samples were used for stable isotope measurements.

After spectral luminescence scanning, the RR2 coral was divided into smaller pieces (numbered #1-7) of approximately 4 to 6 centimetre with a precision rock saw to fit the chamber of the laser. The segments were cut diagonal to get an overlapping transect. After cutting the coral segments they were cleaned in a Milli-Q water bath and dried for 24 hours.

A small part of the RR2 coral slab (RR2#2) was used for method development of trace element and stable isotope measurements. Samples were obtained as described above.

3.4. Stable isotope ratio measurements

The stable isotopic composition of the coral carbonate was measured using a Finnigan MAT 253 mass spectrometer connected to a KIEL IV carbonate preparation device at the NIOZ research institute (Texel, Netherlands). For each sample, 20 to 40 µg of powdered material was used. The powdered material was reacted with phosphoric acid (H_3PO_4) at a temperature around 70°C producing CO_2 gas. The isotopic composition of the gas was measured by a mass spectrometer. Two international standards were measured along with the samples: NBS-19 and VICS. The target value for the VICS standard of -5.44‰ is similar as the values for coral $\delta^{18}O$, which makes it a suitable standard for the $\delta^{18}O$ measurements. The standard deviation of multiple analyses for VICS and NBS-19, respectively N=20 and N=16, were ±0.03‰ and ±0.06‰ for $\delta^{18}O$ and ±0.04‰ and ±0.04‰ for $\delta^{13}C$. All values were measured relative to the Vienna Peedee belemnite (VPDB) standard. The sample data was finally resampled to monthly data points by using AnalySeries (Version 1.1.1, Paillard et al., 1996).

3.5. Seawater $\delta^{18}O$ reconstruction

The $\delta^{18}O$ stable isotope ratio measurements of the coral aragonite is a function of both sea surface temperature (SST) and seawater $\delta^{18}O$ composition ($\delta^{18}O_{SW}$) (Equation 1; Ren et al., 2003):

$$\Delta\delta^{18}O_{(coral)} = \Delta\delta^{18}O_{(SST\ contri)} + \Delta\delta^{18}O_{(SW\ contri)} \quad \text{(Ren et al., 2003)} \tag{1}$$

The resampled and interpolated monthly data of the $\delta^{18}O$ measurements, based on the G/B ratio age model was used to construct the $\delta^{18}O_{SW}$ of the different coral slabs. The method by Ren et al. (2003) isolates $\delta^{18}O_{SW}$ from the coral $\delta^{18}O$ by breaking the monthly changes of coral $\delta^{18}O$ into separate contributions of SST and $\delta^{18}O_{SW}$. Different approaches were used to find the best method for reconstructing the $\delta^{18}O_{SW}$. Besides the Sr/Ca ratio measured by the HR-ICP-MS (Thermo Scientific ELEMENT-2) (data provided by Pascher, 2012), also the reconstructed sea surface temperatures of monthly field observations [see *3.8.2. Sea Surface Temperature*] have been used as a SST proxy for the Berau delta system. The impact of SST on biologic carbonate is determined to be varying between -0.15 and -0.22‰ C^{-1} (Ren et al., 2002, Suzuki et al., 2005). For this study, a value of -0.21‰ C^{-1} was used, based on previous measurements in the Berau delta system (Pascher, 2012). Both methods were applied on the RR2 core, as this core is expected to give the highest amplitude in salinity fluctuation due to its location in the Berau delta system.

3.6. Trace elements method development

Different measuring methods were used to calculate trace element ratios, as they were tested on a small part of the RR2 coral (RR2#2) in order to select the best measuring method. The RR2#2 coral slab was chosen for this method development due to the high expected differences in salinity as a result of the location of the coral and the occurrence of the 1997-1998 El Niño event in this part of the coral slab. Besides line-scans and line of spot scans with the Laser Ablation ICP-MS, also powdered material was used for Sector Field ICP-MS measurements. The results of the different methods were compared to each other, to the trace element data constructed by the research of Pascher (2012), and to the results of the G/B ratio, $\delta^{18}O$, and calculated $\delta^{18}O_{sw}$ values.

3.6.1. Sector Field ICP-MS (Thermo Scientific Element-2)

Before analyses by ICP-MS, 0.5 to 1 mg of the powdered RR2#2 material was dissolved in ultrapure 0.1M HNO_3 and stored in 5ml vials. The 23 obtained samples were dissolved by using a Vortex mixer

until all material was dissolved. The diluted samples, together with the JCp-1 standards and blanks, were measured with a Sector Field ICP-MS (Thermo Scientific Element-2) at the NIOZ research institute (Texel, Netherlands). Elements measured with this technique were Na, Mg, Ca, Sr, and B. Accuracies for the JCp-1 standard were 103% (Mg), 105% (^{88}Sr), 104% (^{87}Sr), 99% (Na) and 86% (Ba). Results were resampled with AnalySeries (Version 1.1.1, Paillard et al., 1996) to a monthly dataset by using the through G/B-derived age model.

3.6.2. Laser Ablation ICP-MS linescan and line of spots

A linescan was performed parallel to the major growth axis of the RR2#2 coral slab. The coral slab was pre-ablated with a scanspeed of 40µm/s to expose fresh material for analysis. Laser beam settings were altered to obtain the best possible settings for measuring the whole coral slab. The resulting settings for these measurements are given in Table 3. Before and after every 5mm of coral slab the reference material MACS3, NIST 610, NIST 612, JCt and JCp were measured to correct the results for drift. The amount of measured elements was reduced to a minimum to obtain a higher reliability of the results (Table 3). Ratios were obtained for all the measured elements, relative to the ^{43}Ca intensities. The resulting ratios were smoothed with Matlab (Version 9.0, Mathworks) and a monthly dataset was obtained with AnalySeries (Version 1.1.1, Paillard et al., 1996) by using the through G/B-derived age model.

Besides a linescan, also a line of spots Laser Ablation ICP-MS was conducted on the RR2#2 coral slab. Settings were chosen so that the time for measuring the whole coral slab was equal to the time of the linescan, in order to keep the results broadly equal. The coral slab was pre-ablated with a speedscan of 40µm/s, equal to the linescan measurements, to expose fresh material for analysis. Also reference material and measured elements were kept equal to the linescan measurements. The spot size of the line of spot scan was set to the maximum size (120 µm) to reduce the noise of the non-homogeneous coral material. Results were resampled with AnalySeries (Version 1.1.1, Paillard et al., 1996) to a monthly dataset by using the through G/B-derived age model.

3.6.3. Method used for trace element measurements

Results of the different measuring techniques were compared to each other, to the other trace element data of RR2 by Pascher (2012), and to the G/B ratio, $\delta^{18}O$, and calculated $\delta^{18}O_{sw}$ values of the same coral slab. Due to the constant results in trace elements to Ca ratio, the best correlation with the other proxies, and the relative low time-consuming process of the Laser Ablation ICP-MS linescan, this method was used to measure trace elements for the whole RR2 coral slab. The settings were optimized and are given in the table below (Table 3). Due to the limited space in the chamber of the Laser Ablation ICP-MS, the seven pieces of RR2 coral core were measured in two different series. The boundary between the two different sets is located at a depth of 116mm, corresponding to approximately November 1987 based on the through G/B-derived age model.

	Settings
Used method	Laser Ablation ICP-MS Linescan
Measured coral	RR2
Reference material	MACS3, NIST610, NIST612, JCt, JCp
Scanspeed	10 µm s^{-1}
Pre-ablation scanspeed	40 µm s^{-1}
Energy density	1 J cm^{-2}
Repetition rate	10 Hz
Spot size	20 µm to 150 µm
Measured elements	^{23}Na, ^{24}Mg, ^{27}Al, ^{43}Ca, ^{88}Sr, ^{138}Ba

Table 3. Final settings of the trace element measurements for the RR2 coral slab.

The results of the Trace element measurements will be compared to previous research analysis (Table 4) and the data of climatic indices, and together with the G/B ratio and stable isotope measurement they will be used to reconstruct the environmental variability in the research area.

Element/Ca ratio	General range [mmol/mol]	References
Na/Ca	15-24	Mitsuguchi et al. (2010)
Mg/Ca	2.5-6.5	Mitsuguchi et al. (2010)
Al/Ca	0.1-3	Wang et al. (2011), Pascher (2012)
Sr/Ca	8.0-10.0	Mitsuguchi et al. (2010)
Ba/Ca	0.0027-0.016*	McCulloch et al. (2003), Sinclair and McCulloch (2004), Pascher (2012)

*Table 4. Measured trace elements to calcium ratios of previous researches. *Ba/Ca values in the top of the coral cores can extend up to 0.1 mmol/mol.*

3.7. Coral chronology

The age models for the coral cores are based on the seasonal cycles of the G/B ratios. 12 of the 24 coral slabs (see Table 2) that were measured with SLS showed a clear cyclicity. These 12 coral slabs were used for a consistent climate-based age model. G/B maxima values were assigned to the highest expected river outflow based on precipitation data, as well as model and observational data for the river plume dynamics as shown in Tarya et al. (2015) and Tarya et al. (in preparation). An X-ray was made of the RR2 coral slab to see if the density, and thereby the growth rate of the coral was constant (Figure 8). No major differences in density where found in the coral so that a linear interpolation was made between the fixed annual peaks of the G/B ratios by using AnalySeries (Version 1.1.1, Paillard et al., 1996). This resulted in a monthly age model for all 12 of the coral slabs. The G/B ratio age models were compared to each other and were also transferred to the trace element and stable isotope measurements.

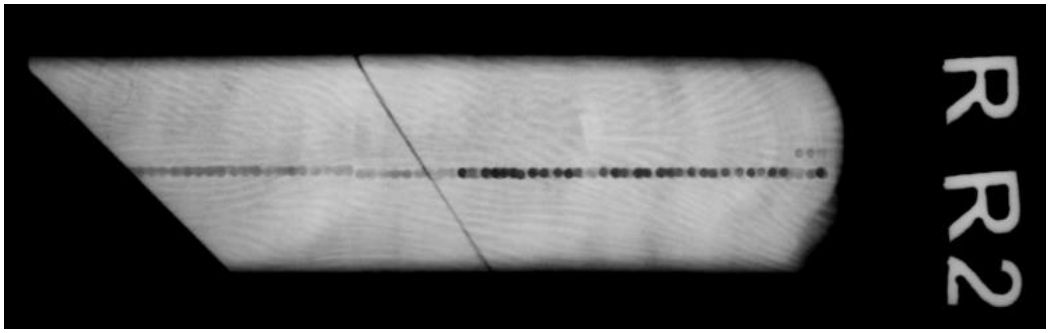

Figure 8. Inverge image of the X-ray of RR2#1 (right) and RR2#2 (left). Used to measure the difference in density of the coral for constructing the age model. The coral was irradiated for 20sec with an energy of 50kV.

3.8. Metadata

To observe the influence of interannual to decadal climate variability on the environment of the Berau delta, the obtained data was compared to different climate indices and datasets. The Climate Explorer database provided by the Royal Dutch Meteorological Institute (KNMI; climexp.knmi.nl) was used for most of these datasets. This database was also used for the construction of anomalies of the different datasets to remove seasonal signals from the data and calculating the correlation (r) of the climate indices to the anomalies of the different measured proxies. The Morlet Wavelet Power Spectrum of Torrence and Compo (1998) was used to analyse variations of frequency within time series.

3.8.1. El Niño-Southern Oscillation

The database used to visualize the ENSO [see *2.3.2. El Niño-Southern Oscillation*] is the monthly HadISST1 Nino3.4 index (KNMI; climexp.knmi.nl). The ENSO index is defined by the anomalies of the average SST for the region in the middle of the Pacific Ocean, between -170 to -120 degrees longitude and -5 to 5 degrees latitude. The anomalies are normalized to 1971-2000. El Niño and La Niña events for this research are based on a 3 month running average of the Oceanic Niño Index (ONI), with the thresholds for moderate, strong, and very strong El Niño events of respectively 1.0 to 1.4, 1.5 to 1.9 and ≥ 2, and respectively -1.0 to -1.4, -1.5 to -1.9 and ≥ -2 for La Niña events (Null, 2016). The resulting El Niño and La Niña events for a period between 1970 and 2005 are presented in the table below (Table 5). The Nino3.4 index show a negative correlation with the ITF index and a positive correlation with the IOD index, as expected based on previous research [see *3.8.8. Correlation of the different climate indices*] (Liu et al., 2015).

El Niño			La Niña		
Moderate	Strong	Very Strong	Moderate	Strong	Very strong
1986-87	1987-88	1972-73	1970-71	1973-74	
1994-95	1991-92	1982-83	1984-85	1975-76	
2002-03		1997-98	1995-96	1988-89	
			1998-99	1999-00	

Table 5. El Niño and La Niña events since 1970 based on the 3 month running average of the Oceanic Niño Index (ONI) (modified after Null, 2016).

3.8.2. Sea Surface Temperature

Sea surface temperature data was obtained from the NOAA Extended Reconstructed Sea Surface Temperature (ERSST), Version 4 (KNMI; climexp.knmi.nl). This global analysis of sea surface temperature derives monthly data from the International Comprehensive Ocean-Atmosphere Dataset and fills missing data by statistical methods (Huang et al., 2015). The ERSST has a regular grid of 2.00^{o} in both latitude and longitude. The cutting out region used for this research is between 117^{o}E and 121^{o}E longitude and 1^{o}N and 3^{o}N latitude with a minimum of 30 valid points for this region.

3.8.3. Temperature and precipitation

A monthly temperature and precipitation dataset was obtained from the Meteorological and Geophysical Agency station (Badan Meteorologi dan Geofisika - BMG) in Tanjung Redeb (117.47^{o}E 2.15^{o}N) for the period of 1987 to 2007. This station is located at the mouth of the Berau River.

3.8.4. Indian Ocean Dipole

The Dipole Mode Index (DMI) (KNMI; climexp.knmi.nl) is a monthly dataset of the difference between the western equatorial Indian Ocean HadISST1 SST (50^{o}E-70^{o}E and 10^{o}S-10^{o}N) and the south eastern equatorial Indian Ocean HadISST1 SST (90^{o}E-110^{o}E and 10^{o}S-0^{o}N) representing IOD events. A positive DMI refers to a positive IOD event. Most of the extreme IOD events correspond well with major El Niño events (1982 and 1997) although other extreme events (1994) are not noticeable in the Nino3.4 index [see *3.8.8. Correlation of the different climate indices*].

3.8.5. Indonesian Throughflow

For the reconstruction of the ITF, the Eddy-resolving Ocean model reconstruction by van Sebille et al. (2014) was used. The reconstruction model is based on tracking virtual Lagrangian particles in the Connectivity Modelling System v1.1 (Paris et al., 2013). This results in a modelled reconstruction, based on CORE reanalysis products of atmospheric forcing, of the ITF between 1963 and 2002. The resulting anomalies show a negative correlation with the Nino3.4 index (see *3.8.8. Correlation of the different climate indices*).

3.8.6. Pacific Decadal Oscillation

The monthly PDO index based on HadSST3 is the difference in SST between the eastern and north western Pacific Ocean (KNMI; climexp.knmi.nl).

3.8.7. Correlation of the different climate indices

Table 6 shows the correlation between the anomalies of the different climate indices based on the Climate Explorer database (KNMI; climexp.knmi.nl), assuming there was no lag in any of the climate indices.

correlation (r)	ITF	IOD	PDO
Nino3.4	-0.542	0.399	0.474
ITF		-0.114	-0.359
IOD			-0.021

Table 6. Correlation between the anomalies of the most important climate variables for the Berau delta system. Correlations are constructed with the Climate Explorer database (KNMI; climexp.knmi.nl). Note: all correlations were computed assuming there was no lag in any of the data (lag=0).

4. Results

4.1. Green/Blue ratio spectral luminescence scanning

Figure 9 shows the result of the G/B ratios of Spectral Luminescence Scanning (SLS) of 6 of the 12 best preserved and longest coral cores from the Berau delta system. The location of these 6 cores are spread over the Berau delta system, with locations close to shore (RR2 and RR4) and locations up to 50 kilometre offshore (Maratua). Due to the variability in the position of the different cores, the impact of the Berau River on G/B ratio can be observed.

The results of the G/B ratio in Figure 9 show a clear difference between the coral cores close to the coastline (RR2 and RR4) and the cores that are located further away from the coastline. The RR cores show higher G/B ratios (average of 0.94 to 0.81) and an enhanced amplitude (average of 0.11 to 0.05) in respect to the cores located further from the coastline. Besides these differences, all cores show strong seasonal signals. The amplitude of the RR datasets is significantly reduces at some years (1973, 1983 and 1998). These years correspond to the most significant El Niño events. Although less clear, these amplitude reductions are also visible at the cores that are located further offshore. No significant changes in amplitude or power were found during the strong 1988-1989 and 1999-2000 La Niña events.

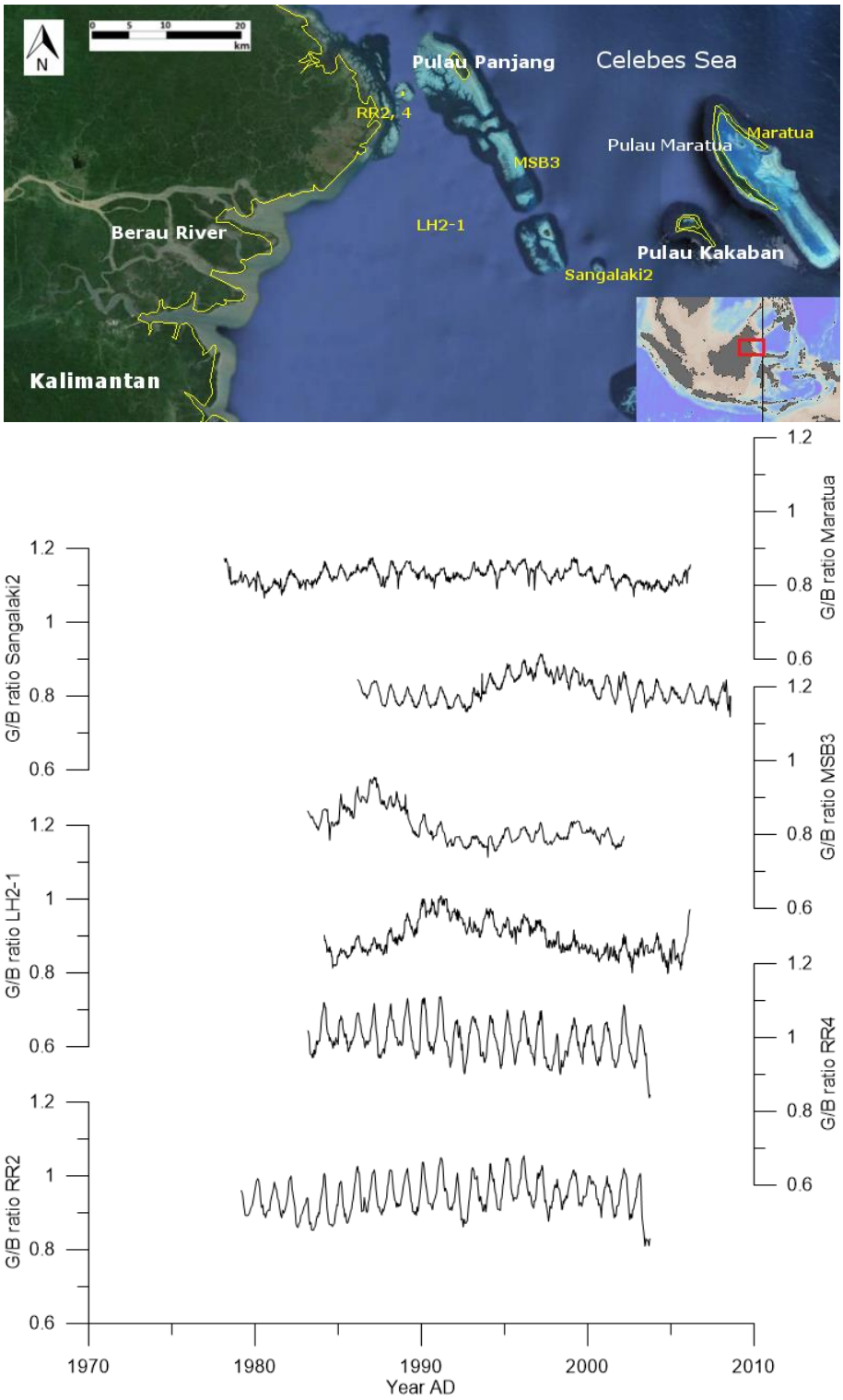

Figure 9. Results of the G/B ratio measurements of the Berau delta system coral cores RR2, RR4, LH2-1, MSB3, Sangalaki2 and Maratua. The locations of these coral cores are given in yellow on the map above. All cores were measured with a 0.5mm average, peaks were correlated to the highest river outflow flux in March. Results were resampled to a monthly resolution.

4.2. Annual growth rate

The annual growth rate of the different coral slabs have been measured based on the G/B ratio constructed age model. The average annual growth rate of the 12 measured coral slabs varied between 10 and 18 mm. The growth rate seems to be independent to the distance of the coral to the shoreline. During strong El Niño and La Niña events the annual growth did not show a large offset in growth rate in respect to the average measured value. Fluctuations within a year are still highly unknown due to the fact that only one correlation point is used per year (i.e. the peak in G/B ratio corresponding to the highest river outflow).

4.3. Coral $\delta^{18}O$

Results of the coral $\delta^{18}O$ of RR4, together with the dataset of previous measured coral $\delta^{18}O$ of RR2, Maratua, LH2_1, MSB3 and Sangalaki are used to make a reconstruction of the $\delta^{18}O_{sw}$ for the Berau delta system. Figure 10 shows the results of the coral $\delta^{18}O$ measurements of these 6 cores.

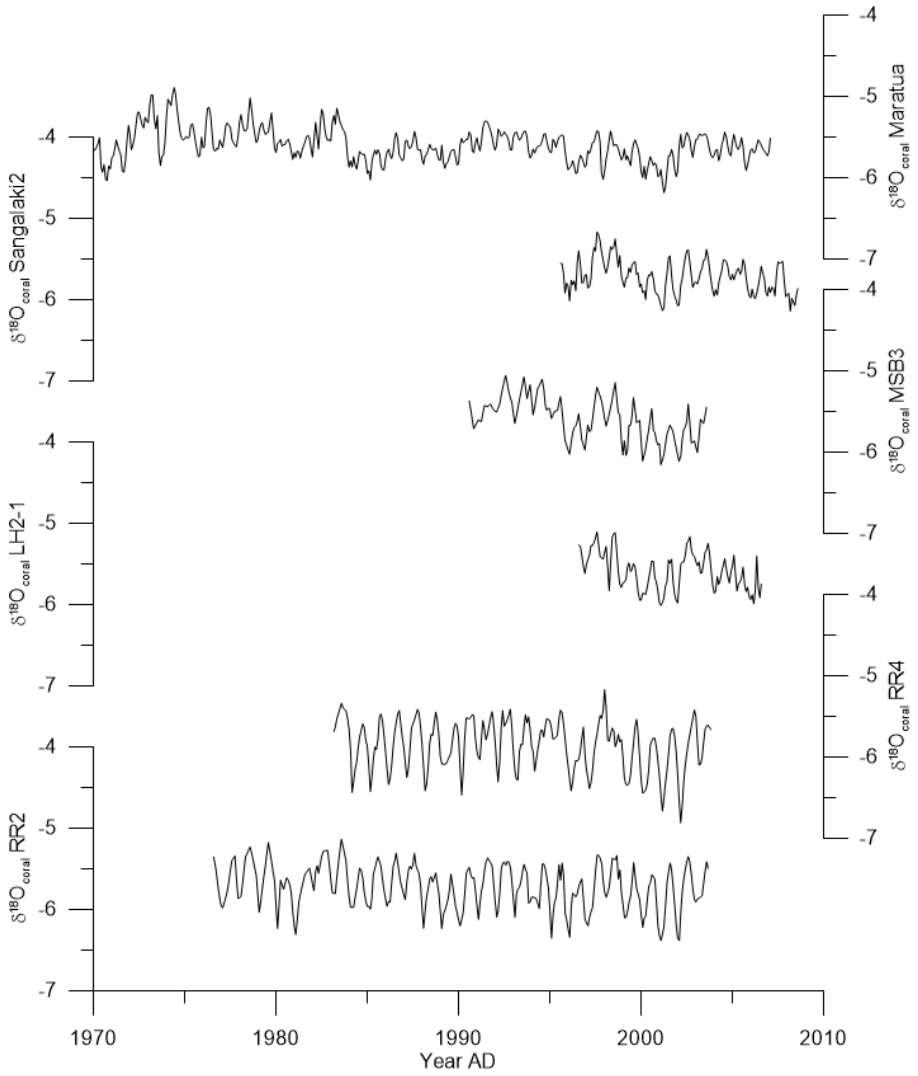

Figure 10. Results of the coral $\delta^{18}O$ measurements by Pascher (2012) [cores RR2, LH2-1, MSB3, Sangalaki2 and Maratua] and this research (core RR4). The locations of these coral cores are given in yellow on the map in Figure 9. Peaks were correlated to the highest river outflow flux in March. Results were resampled to a monthly resolution, based on the G/B age model.

The results of the coral $\delta^{18}O$ show a clear seasonal signal, although these signals are more obvious for the coral cores located close to the shoreline (RR2 and RR4). Also the amplitude (0.68 to 0.35) for these cores is higher and the average values are slightly more negative (-5.78 to -5.62) in respect to the cores located further from the coastline. A few periods with less amplitude and slightly less negative values are observed for most of the coral slabs around 1981 and 1998, corresponding to the strongest El Niño events. These periods are best visible at the close to shore cores. No significant changes in amplitude or power were found during the strong 1988-1989 and 1999-2000 La Niña events.

4.4. Seawater $\delta^{18}O$

Sr/Ca ratio measurements and ERSST data is used for the reconstruction of $\delta^{18}O_{sw}$ to obtain the best possible method of reconstruction (Figure 11). Both methods were applied on the RR2 coral core. Although Sr/Ca ratio is measured at the exact location of the $\delta^{18}O$ measurements and can be used as a direct proxy for SST, the modelled ERSST show a similar pattern and is available for a longer time interval. Furthermore, there is no Sr/Ca data available for all the coral slabs and the data of Sr/Ca ratio is difficult to interpret due to the small seasonal changes in SST for the Berau delta system. Hence, for this research, usage of the ERSST dataset is preferred. The similarity of the ERSST data to the Sr/Ca record (Figure 11) shows that the ERSST data is well representative of the in-situ temperature and thus suitable for $\delta^{18}O_{sw}$ calculation.

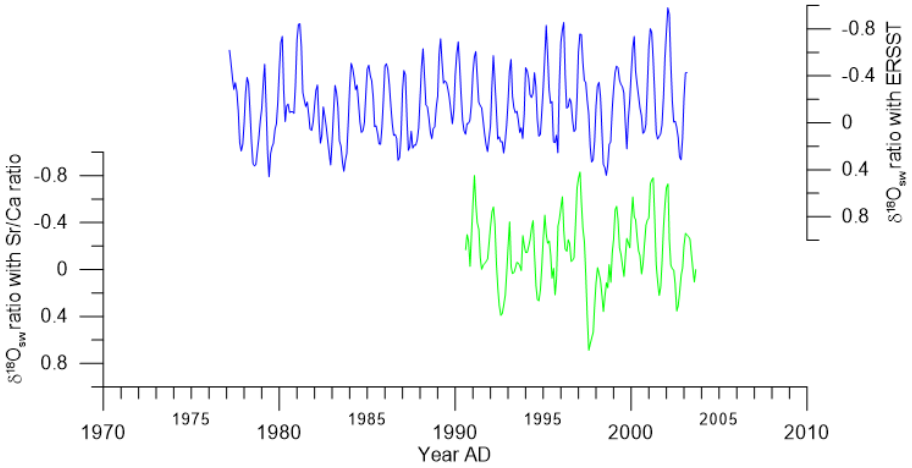

Figure 11. Both methods to calculate the $\delta^{18}O$ of the seawater (Sr/Ca in green and ERSST in blue). Results were resampled to a monthly resolution, based on the G/B age model.

The $\delta^{18}O_{sw}$ of all 6 coral $\delta^{18}O$ records were constructed by using the ERSST data (Figure 12). The age model for the $\delta^{18}O_{sw}$ records are based on G/B ratio.

The results of the reconstruction of $\delta^{18}O_{sw}$ for the 6 Berau coral cores show clear annual cycles, with a decline in cyclicity during the strong El Niño event of 1982-1983 and 1997-1998. These signals are more distinctive for the coral cores close to the shoreline (RR2 and RR4). Similar to the G/B ratio measurements, no distinct change in amplitude is observed during the major La Niña events of 1988-1989 and 1999-2000. Besides that, no clear trend line is visible for any of the records.

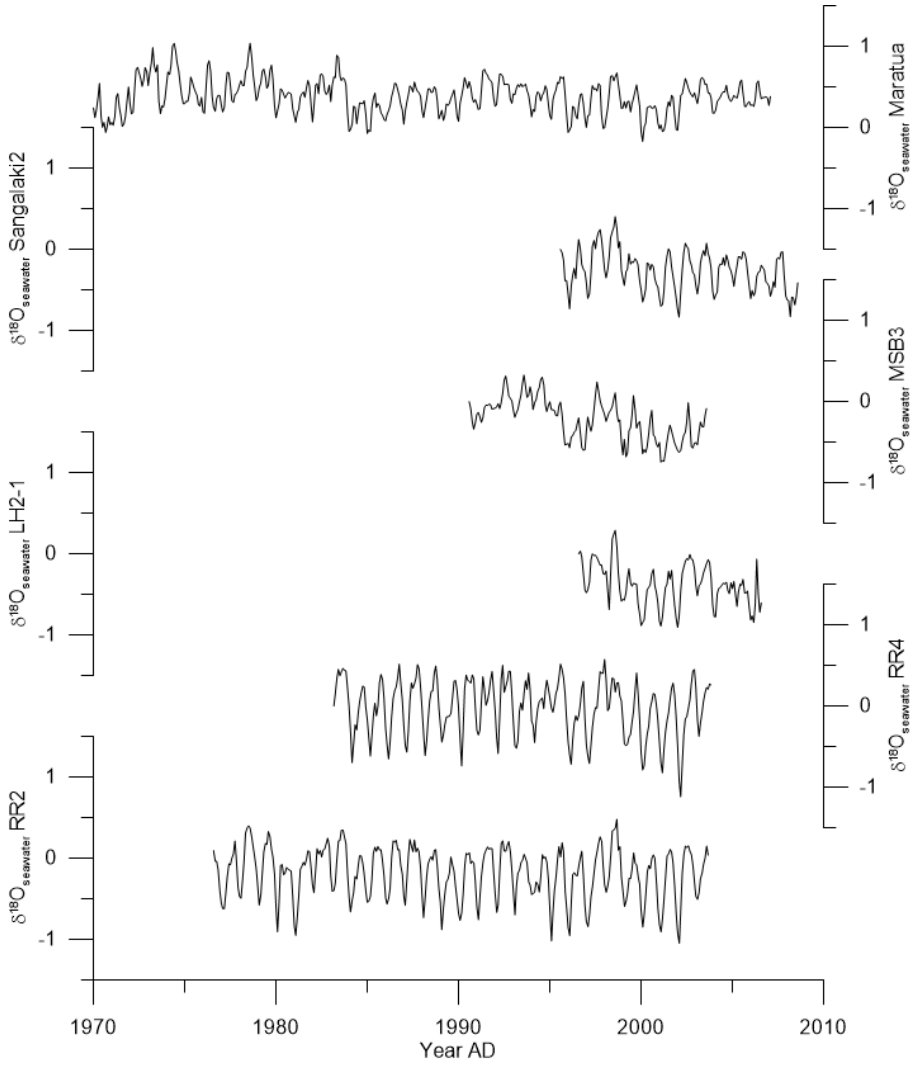

Figure 12. Results of the seawater $\delta^{18}O$ reconstructions by Pascher (2012) [cores RR2, LH2-1, MSB3, Sangalaki2 and Maratua] and by this research [core RR4]. All reconstructions were made by using the ERSST as a measurement for sea surface temperature. The locations of these coral cores are given in yellow on the map of Figure 9. Peaks in coral $\delta^{18}O$ were correlated to the highest river outflow flux in March. Results were resampled to a monthly resolution, based on the G/B age model.

4.5 $\delta^{13}C$

Results of the coral $\delta^{13}C$ of RR4, together with the dataset of previous measured coral $\delta^{13}C$ of RR2, Maratua, LH2_1, MSB3 and Sangalaki by Pascher (2012) are plotted in Figure 13. Peaks of coral $\delta^{18}O$, that was measured with the same sample, were correlated to the highest river outflow flux in March. This age model was used as a $\delta^{13}C$ age model. Results were resampled to a monthly resolution based on the G/B ratio age model.

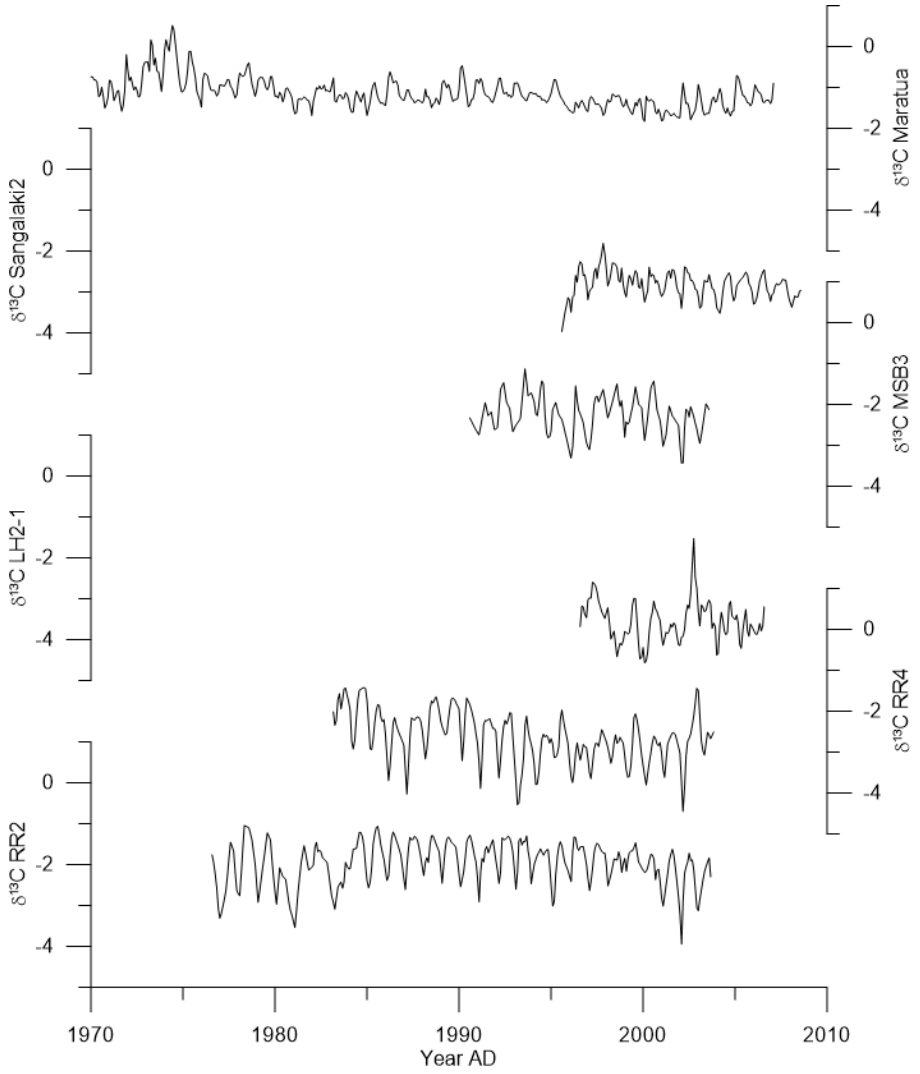

Figure 13. Results of the coral $\delta^{13}C$ measurements by Pascher (2012) [cores RR2, LH2-1, MSB3, Sangalaki2 and Maratua] and this research (core RR4). The locations of these coral cores are given in yellow on the map of Figure 9. Peaks of coral $\delta^{18}O$ that was measured with the same sample were correlated to the highest river outflow flux in March. Results were resampled to a monthly resolution, based on the G/B age model.

The results of the $\delta^{13}C$ show a similar pattern as the $\delta^{18}O_{sw}$ results, with seasonal cycles for all records. These cycles are less clearly recognisable in respect to the $\delta^{18}O_{sw}$ measurements. No clear correlation has been found between the values of $\delta^{13}C$ and the distance to the shoreline, although the Maratua core, that is located furthers from the shoreline, show higher $\delta^{13}C$ values than the other coral cores. The amplitude for close to shore cores is much higher than the cores that are located further away from the shoreline (respectively 1.12 and 0.51).

4.6. Trace elements

Three different methods of trace element measurements are applied on a small part of the RR2 coral (RR2#2) to develop the best suited method. Besides the result of the dissolved powder material (sector field ICP-MS) and two different laser ablation methods (line of spots and linescan), also the ICP-OES results of Pascher (2012) are given in Figure 14. Age models are based on the G/B ratio measurements. All data was resampled to a monthly dataset in order to obtain a similar resolution for all the data.

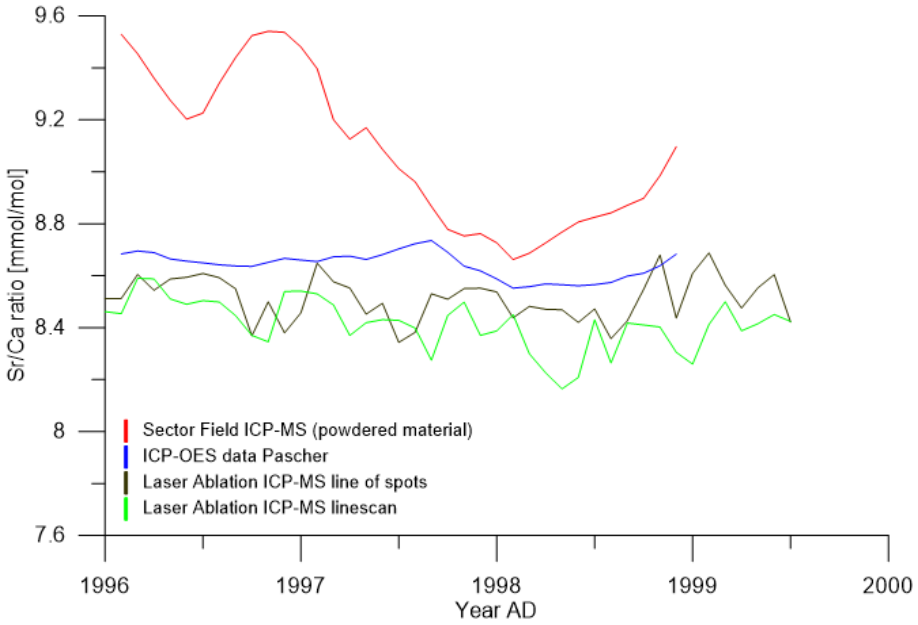

Figure 14. Results of the different methods of trace element measurements of the RR2#2 coral slab. All results were resampled to monthly data to set all datasets in a same resolution. The age model for these methods is based on the G/B ratio data of the RR2 coral core.

The results of the different methods show values of Sr/Ca ratio between 8.2 and 9.6 mmol/mol, which corresponds to the general observed range of Sr/Ca ratio in coral of 8 to 10 mmol/mol (Mitsuguchi et al., 2010). The linescan and line of spots laser ablation results correlate better to the ICP-OES measurements of Pascher compared to the powdered material ICP-MS measurement. A possible reason for the offset in Sr/Ca ratio in the Sector Field ICP-MS is the amount of measured Sr in the coral with this method. These amounts were in some parts of the coral so high during the development of the method, that they could not be detected and the settings of the measurements had to be reduced to gain valuable results. This caused a decrease in accuracy of the measurements (Hathorne et al., 2013). Due to the relative low time-consuming process and the constant and reliable results of the Laser Ablation ICP-MS linescan technique, this method was optimized (for settings, see Table 3) and used for the whole RR2 coral core. The resulting ratios were smoothed with Matlab (Version 9.0, Mathworks) and a monthly dataset was obtained with AnalySeries (Version 1.1.1, Paillard et al., 1996) by using the through G/B-derived age model. Results of the five measured trace elements to calcium ratios are given in Figure 15. Two graphs are given for the Ba/Ca ratio due to the high concentrations of barium in the upper (living) part of the coral.

The ratios of the different trace elements show similar values compared to the results of previous measured coral trace elements to calcium ratios (Table 4). Although all data have been corrected for drift, the Na/Ca and Mg/Ca ratio data still seems to show a drift. The data has a decreasing trend until it reaches a minimum around the year 1988. From here on, there is an increasing trend in the ratio. The tipping point of this drift is exactly at the boundary between the two different sets of measurements.

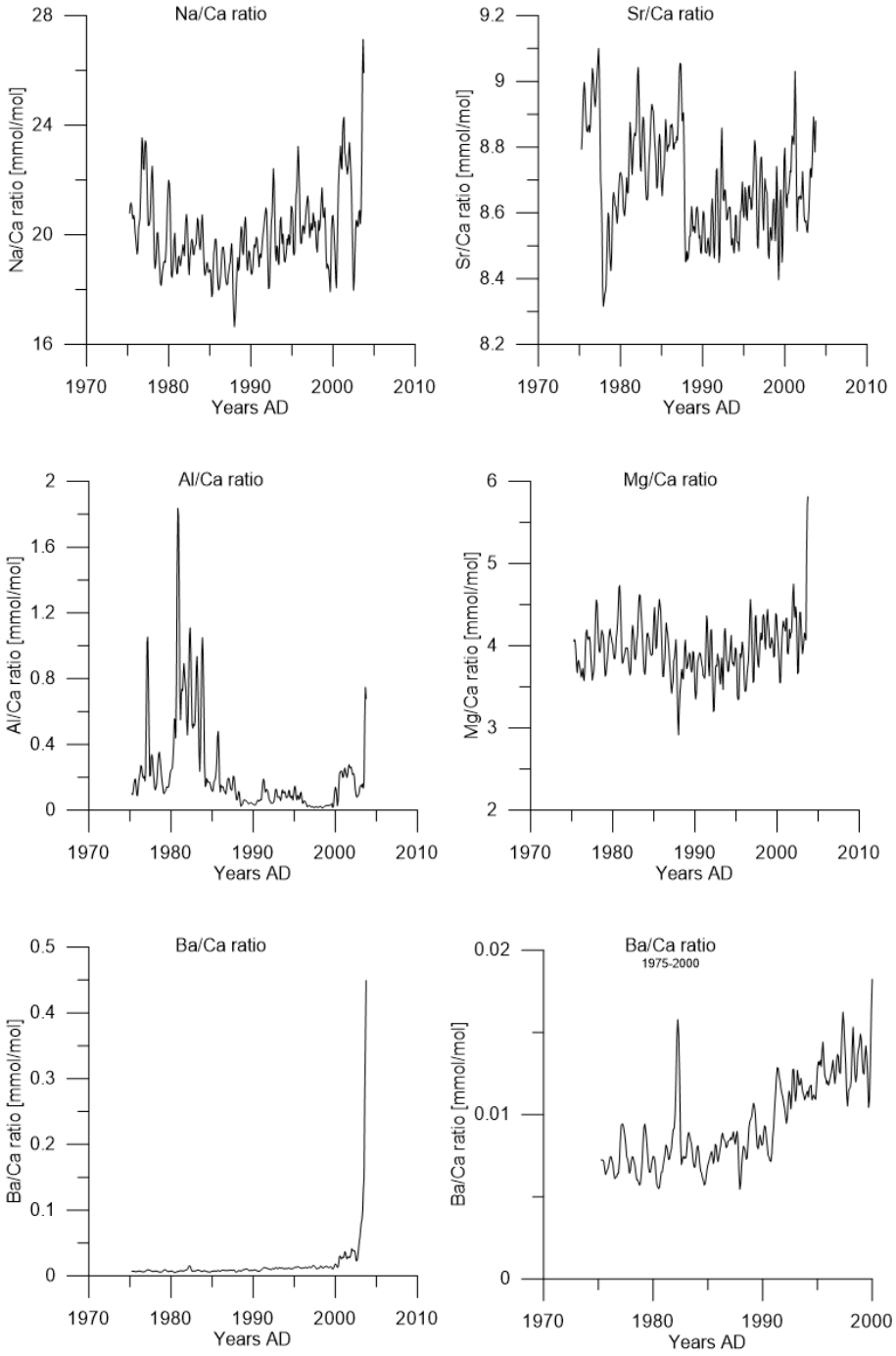

Figure 15. Results of the RR2 coral slab trace element analysis with Laser Ablation ICP-MS Linescan. Data is smoothed by using Matlab and resampled to a monthly dataset based on the G/B ratio age model.

For the Sr/Ca ratio, some extreme transitions are noticeable at 1977-78, corresponding to the transition of RR2#6 and RR2#7, and at 1987-88. This last transition is at the same depth as the transition or RR2#4 and RR2#5, the boundary between the two different sets of measurements. In the second part of the measurements, from 1988 onwards, the Sr/Ca ratio seems much more constant although a slight increasing trend is visible. For the Al/Ca ratio, high levels are observed in the oldest part of the coral slab before 1985. As a possible proxy for contamination, these high values correspond well with black spots in the G/B ratio image of the RR2 core (Figure 7b). Also in the last few centimetres of the RR2 coral slab, high values of Al/Ca are found. Only between 1985 and 2000, levels of Al/Ca ratio

are steady and low (below 0.2 mmol/mol). For the Ba/Ca ratio an upward trend is found in the data. Especially in the last few centimetres (since 2000) levels are increasing exponentially. A peak in Ba/Ca ratio is observed in 1982, corresponding to a major El Niño event.

Only Na/Ca and Mg/Ca show seasonal cycles in their data (Figure 16). Na/Ca ratio show a minimum value of 19.66 mmol/mol in the month May and a maximum value of 20.63 mmol/mol in October. This is an amplitude of 5.0 percent for the annual periodicity. For Mg/Ca the minimum values is reached in March with 3.8 mmol/mol where 4.1 mmol/mol is established in October. This is a percentage difference of 7.4 for the annual periodicity amplitude.

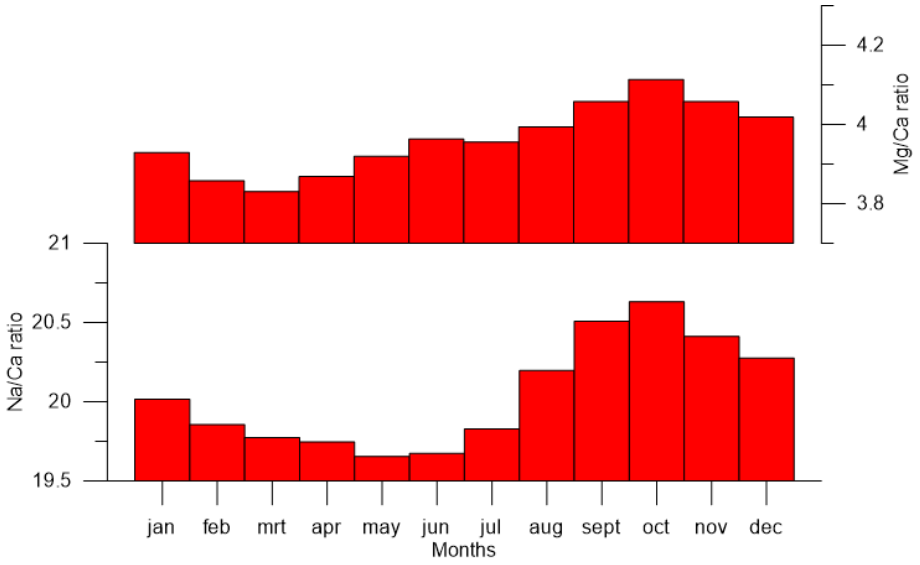

Figure 16. Monthly averages for the Na/Ca (below) and Mg/Ca (above) ratios of the RR2 coral core.

5. Discussion

5.1. Conventional proxies

Higher amounts and higher fluctuations in river runoff are expected close to the river mouth due to a higher impact of the Berau River for these corals. The stronger changes in amplitude and higher amounts of the different conventional proxies (i.e. G/B ratio, $\delta^{18}O_{sw}$) for the close to shore RR cores strengthen the theory that these are valuable proxies for river runoff and oceanic salinity.

Due to the differences in amounts and fluctuations for the close to shore and distant coral cores for the conventional proxies, the RR cores that are located close to the shoreline were combined. A combination has also been made for the cores that are located further offshore (DER-E4, LH2-1, MSB2, MSB3, Sangalaki2, SL3 and Maratua). This was done to correct for local effects and reconstruct a regional signal of river discharge. The combined datasets of both $\delta^{18}O_{sw}$ and G/B ratio were compared to the Nino3.4 index and the DMI (IOD index) (Figure 17), as these indices have a major impact on the research area (Table 7). Anomalies of the data were used to focus on interannual climate variability. The $\delta^{18}O_{sw}$ records of the distant coral cores are generally very short and have no data in the timeframe before 1985. For this reason, the distant coral cores $\delta^{18}O_{sw}$ (red in Figure 17) are only represented by the coral core data of the Maratua slab before 1985.

The amplitude of the G/B ratio anomalies (Figure 17) is very limited and although peaks and lows in this data are corresponding to the peaks and lows in the Nino3.4 index, also a clear drift in the data is observed. Before 1988 the ratio is decreasing, where it is increasing after 1988. This drift is found for both close to shore and further offshore datasets. A possible cause for this drift in G/B ratio is the rapid decrease of rainforest in the Berau district, and the resulting increase in soil erosion and sediment fluxes towards the Berau Delta (Buschman et al., 2012). For $\delta^{18}O_{sw}$ no such drift is found, probably because this is not a proxy for the amount of terrestrial soils of river runoff.

Both $\delta^{18}O_{sw}$ and G/B ratio records show a clear correlation with the Nino3.4 index and the DMI (Figure 17). The 5 year running correlation shows that this correlation is not constant over time. During some periods the correlation between the measured anomalies and the climate anomalies is reduced or even lacking. To get a better understanding in the correlation between the conventional proxies and the climate indices, a 2 year running correlation was constructed for the close to shore coral records (KNMI; climexp.knmi.nl) (Figure 18). Major El Niño events and La Niña events are indicated for comparison.

Where the $\delta^{18}O_{sw}$ 2 year window running correlation shows peaks during both major El Niño and La Niña events, the G/B ratio 2 year window running correlation only show a good correlation during El Niño events. During La Niña events, almost no correlation was found. Although these results are very constant over time and were found for all events, the occurrence of small offsets is very plausible for this small window range.

Still, the difference in the correlation for both $\delta^{18}O_{sw}$ and G/B ratio with La Niña events can be caused by the high precipitation during normal conditions in the Berau delta system. Under these normal conditions precipitation and erosion are very high. If a La Niña events occurs, the amount of precipitation increases, resulting in higher runoff of the Berau River. This will result in a lower salinity, which will be visible in the $\delta^{18}O_{sw}$ record. The G/B ratio is used as a proxy for river runoff by calculating

the amount of soil that is distributed to the ocean. An increase in precipitation does not necessarily need to cause an increase in erosion and thus sediment supply for the Berau River (Morgan, 2009). The rate of erosion is not only described by the amount of precipitation, as well as the intensity of the precipitation. Short and heavy precipitation results in much more erosion compared to long and moderate precipitation (Morgan, 2009). In conclusion, La Niña events are only affecting the amount of river runoff, and not necessarily the amount of sediment supply. It is thereby expected that the $\delta^{18}O_{sw}$ record will give a better representation of the Berau River runoff in respect to the G/B ratio record.

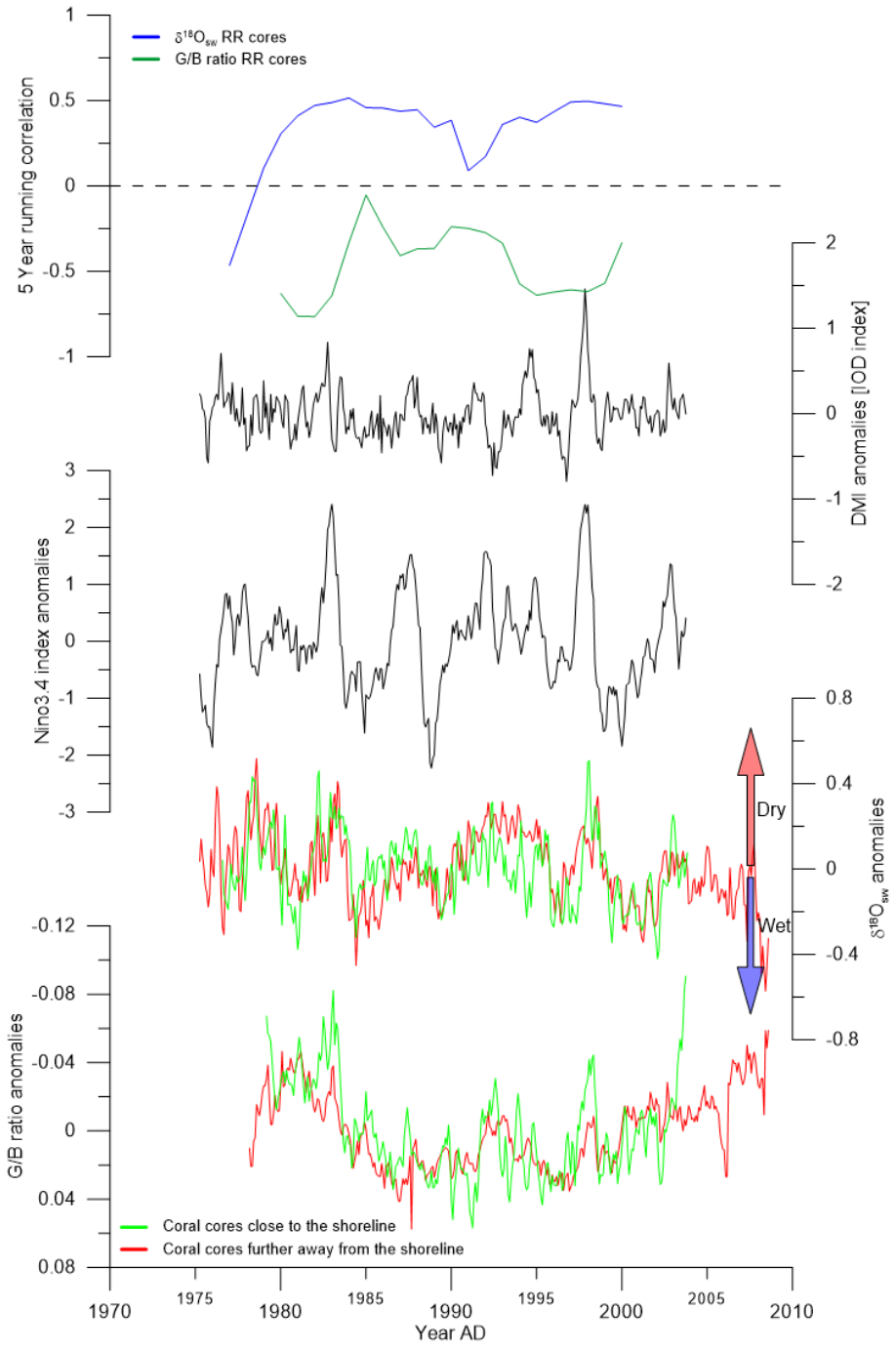

Figure 17. Correlation between G/B ratio, $\delta^{18}O_{sw}$, Nino3.4 index and the DMI (IOD index). All four graphs show anomalies to correct for seasonal cycles. For both $\delta^{18}O_{sw}$ and G/B ratio, the close to shore cores are combined (for G/B: RR NE 1B, RR2, RR4 and RR5, for $\delta^{18}O_{sw}$: RR2 and RR4), as well as the cores located further away from the shoreline (for G/B: DER-E4, MSB2, MSB3, Sangalaki2, SL3 and Maratua, for $\delta^{18}O_{sw}$: LH2-1, MSB3, Sangalaki2 and Maratua), in order to reduce the error. Axes are chosen so that correlations of the different anomalies are in the same direction. The upper graph shows the 5 year running correlation between both RR cores ($\delta^{18}O_{sw}$ and G/B ratio) and the Nino3.4 index anomalies.

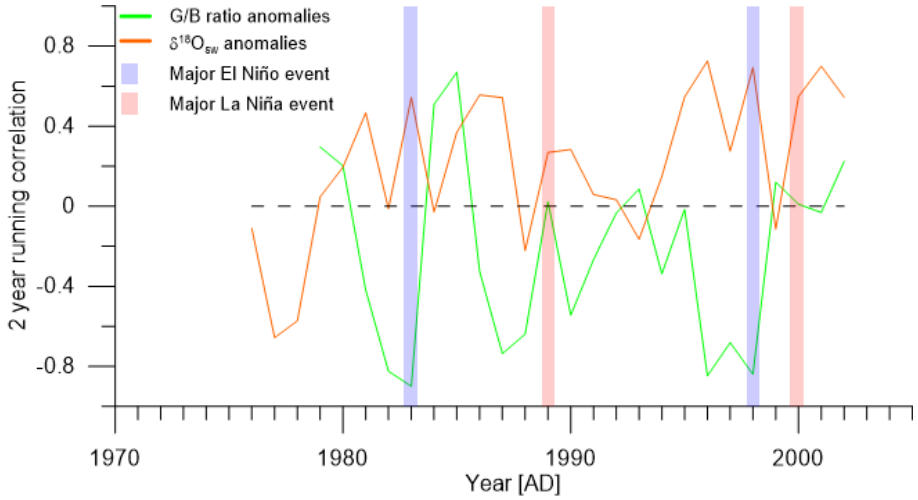

Figure 18. A 2 year running correlation between both the G/B ratio (green) and $\delta^{18}O_{sw}$ (orange) anomalies with the Nino3.4 index anomalies. The correlation is based on the close to shore coral records. The blue and red bars indicate the 2 most important El Niño and La Niña events during the time period.

Data of all G/B, $\delta^{18}O_{sw}$ and $\delta^{13}C$ records were correlated with the 4 major climate indices affecting the Berau delta system by using the Climate Explorer database (KNMI; climexp.knmi.nl). The correlations in Table 7 are based on the anomalies of the measured data and the anomalies of the climate indices. Anomalies were used to focus on interannual climate variability. To correct for the local effect, close to shore and distant coral cores were combined.

River runoff is expected to be high during heavy precipitation in the Berau catchment area. Precipitation is increased during a La Niña event (Glantz, 2001), which corresponds to negative Nino3.4 anomalies. The G/B ratio is used as a proxy for river runoff, and is expected to have a negative correlation with the Nino3.4 index. $\delta^{18}O_{sw}$ on the other hand is used as a proxy for salinity and is expected to have high anomalies when precipitation is low and runoff is decreased. This is related to dry, El Niño events and high Nino3.4 anomalies. So, it is expected that $\delta^{18}O_{sw}$ will have a positive correlation with the Nino3.4 index.

Correlation (r)	Nino3.4	ITF (van Sebille)	IOD	PDO
G/B RR NE 1B, 2, 4 & 5	-0.452	0.374	-0.167	-0.300
G/B Maratua, MSB3, SL3, DER-E4, MSB2 and Sangalaki2	-0.507	0.439	-0.088	-0.255
$\delta^{18}O_{sw}$ RR2+RR4	0.345	-0.211	0.167	0.247
$\delta^{18}O_{sw}$ Maratua, LH2_1, MSB3, Sangalaki	0.408	-0.393	0.145	0.151
$\delta^{13}C$ RR2+RR4	-0.242	0.131	-0.228	-0.025

Table 7. Correlation (r) of the anomalies of the G/B ratio, $\delta^{18}O_{sw}$ and $\delta^{13}C$ reconstructions and the anomalies of the different climate variabilities affecting the Berau delta system. Correlations are constructed with the Climate Explorer database (KNMI; climexp.knmi.nl). Note: all correlations were computed assuming there was no lag in any of the $\delta^{18}O_{sw}$ data (lag=0).

All records display the best correlation with the Nino3.4 index (Table 7). A negative correlation is found for the G/B ratio where the correlation between the Nino3.4 index and the $\delta^{18}O_{sw}$ data is positive. The correlations found with the measured data correspond well with the expected correlations. The correlation between both the ITF and the PDO is not as strong as the Nino3.4 correlation, but is definitely there. As expected, the correlation of the ITF is opposite to the correlation with the Nino3.4 and the PDO (Table 6). The correlation between the IOD and the different reconstructed anomalies is very weak.

The correlation of $\delta^{13}C$ with the different climate indices seems to be less obvious relative to the G/B ratio and $\delta^{18}O_{sw}$ data (Table 7). A possible cause for this low correlation is the impact of other environmental and physiological factors that affects the signal of the $\delta^{13}C$ ratio (Watanabe et al., 2002). Although the anomalies of the $\delta^{13}C$ do not show a good correlation with any of the climate indices, the seasonal cycles are clearly visible (Figure 13). This seasonal cyclicity is higher for the close to shore coral cores in respect to the distant coral cores (respectively amplitude of 1.12 and 0.50). All cores show a minimum in $\delta^{13}C$ at February or March, with the exception of the Maratua core, which is located further offshore. This increases the probability for $\delta^{13}C$ to be a possible proxy for salinity as this seasonal signal is also found in other salinity proxies (i.e. $\delta^{18}O_{sw}$ and G/B ratio). Still, no good correlation with any of the climate indices could be made, and most likely, the $\delta^{18}O_{sw}$ is a better proxy for river runoff compared to the $\delta^{13}C$ data.

The correlation between the different datasets and the ITF anomalies are better for the coral cores that are located further offshore (Table 7). It is expected that fluvial processes have less impact on these coral cores (Tarya et al., 2015) and that oceanic processes such as the ITF are more important at these locations. For the PDO, IOD and Nino3.4 index correlations, no clear difference in correlation was found between close to shore and distant coral cores.

As the Nino3.4 index seems to be the most important factor influencing the Berau delta system, and the Nino3.4 index is highly related to the precipitation pattern in the Berau catchment area, precipitation seems to be more important to the coral formation in respect to ocean circulation (ITF), although the precipitation effect on the distant coral cores is less obvious.

In conclusion, the correlation between the $\delta^{18}O_{sw}$ and G/B ratio with the different climate indices, show a good correlation with the ITF and PDO and especially with the Nino3.4 index. No clear correlation was found with the IOD index. The coral of the Berau delta system seems to give a good representation of the climatic (i.e. salinity) variability in the area. The Nino3.4 index is expected to be the most important factor for the Berau delta system as it influences the precipitation and so the Berau River runoff. Besides that, the higher amplitude of close to shore cores for G/B ratio, $\delta^{18}O_{sw}$ and $\delta^{13}C$ is observed as expected due to the higher impact of the Berau River for these cores. It seems that the Berau River has a high impact on the formation of the coral, not only close to the shore, but even for the Maratua core, 50 kilometres away from the shoreline. Although, the ITF seems to be of more importance on the distant coral cores, as the river runoff for this location is reduced. As a conclusion, the reconstruction of the salinity based on trace element Na/Ca ratio can give a good reconstruction as well.

5.1.1. Limitations conventional proxies

The G/B ratios of the 10 measured coral cores show clear annual banding and are therefore perfectly suited for constructing an age model for the other proxies. Although the annual banding is very clear, extreme climate events such as El Niño can decrease the visibility of the bands. By using very long coral records there is the potential to get an offset in the age model due to these strong climate events. Although strong climate events can impede the process of age modelling, they could also help in the construction of the age model as they can be extra control points in the dataset.

Not all coral cores showed a clear annual cyclicity in G/B ratio. For this research only 50% (12 out of 24) of the coral cores could be used for age modelling. Only 10 of the G/B ratio reconstructions were used for the correlations with climate indices due to the high fluctuation and drift of 2 of the G/B ratio results. If the influence of the river plume is decreased, there is the possibility that making an age model based on G/B ratio is not suitable because the annual banding of the coral cores will be lacking.

Due to the strong impact of the river plume on the G/B ratio, only 1 correlation point could be used for the construction of the age model. The peak in G/B ratio was related to the highest expected runoff based on precipitation and river plume modelling. This peak was set to 1 march although the peak will fluctuate in real life scenario which will create an offset in the age model up to a few months.

The interpolation of the age model is based on a linear growth rate of the coral. While the seasonality in the Berau delta system is very low, it is expected that the growth rate of the *porites* spp. is not constant. This creates a possible offset in the age model up to a few months.

All these factors give a margin of error for the age model for this research in the order of a few months, so that the seasonal signal can be reduced and correlations with other proxies and climate indices can be scaled down.

5.2. Trace elements proxies

The results of the trace elements for the Berau delta system are not as fast-forward as the results of the conventional proxies. Na/Ca and Mg/Ca ratios are the only elements that show clear seasonal cycles. Mg/Ca is often used as a proxy for SST, but due to the fact that there is almost no SST change in the area, it is more likely that SSS is the most important factor that is affecting the Mg/Ca ratio in the coral (Moreau et al., 2015).

If both Mg/Ca and Na/Ca ratios reflect the salinity of the Berau delta system, it is expected that the ratios have a minimum amount during the peak outflow of river runoff around March (Figure 16). The results of the monthly average values of the Na/Ca and Mg/Ca ratios show a minimum value for Mg/Ca around March and for Na/Ca around May. Maximum values of both ratios occur in October. The minimum values correlate well with the expected low salinity level due to the input of fresh water from the Berau River (Tarya et al., 2015).

The anomalies of the trace element measurements were used to correlate the data to the conventional proxy data and the different climate indices (Figure 19). Only the Mg/Ca and Na/Ca ratios are displayed in the figure, as the other trace elements do not show any clear correlation with the climate indices. Al/Ca and Ba/Ca ratios show some extreme high values, probably caused by contamination of the coral

material. Although Sr/Ca shows an unknown cyclicity, it is difficult to correlate this cyclicity with any of the climate indices due to occurrence of some extreme sudden transitions in the data (Figure 15).

The drift in the Mg/Ca and Na/Ca ratios that was found in the raw data (Figure 15) is still found in the anomalies data (Figure 19). Although both trace elements show a seasonal cyclicity, no clear correlation has been found with the climate indices and the conventional proxies.

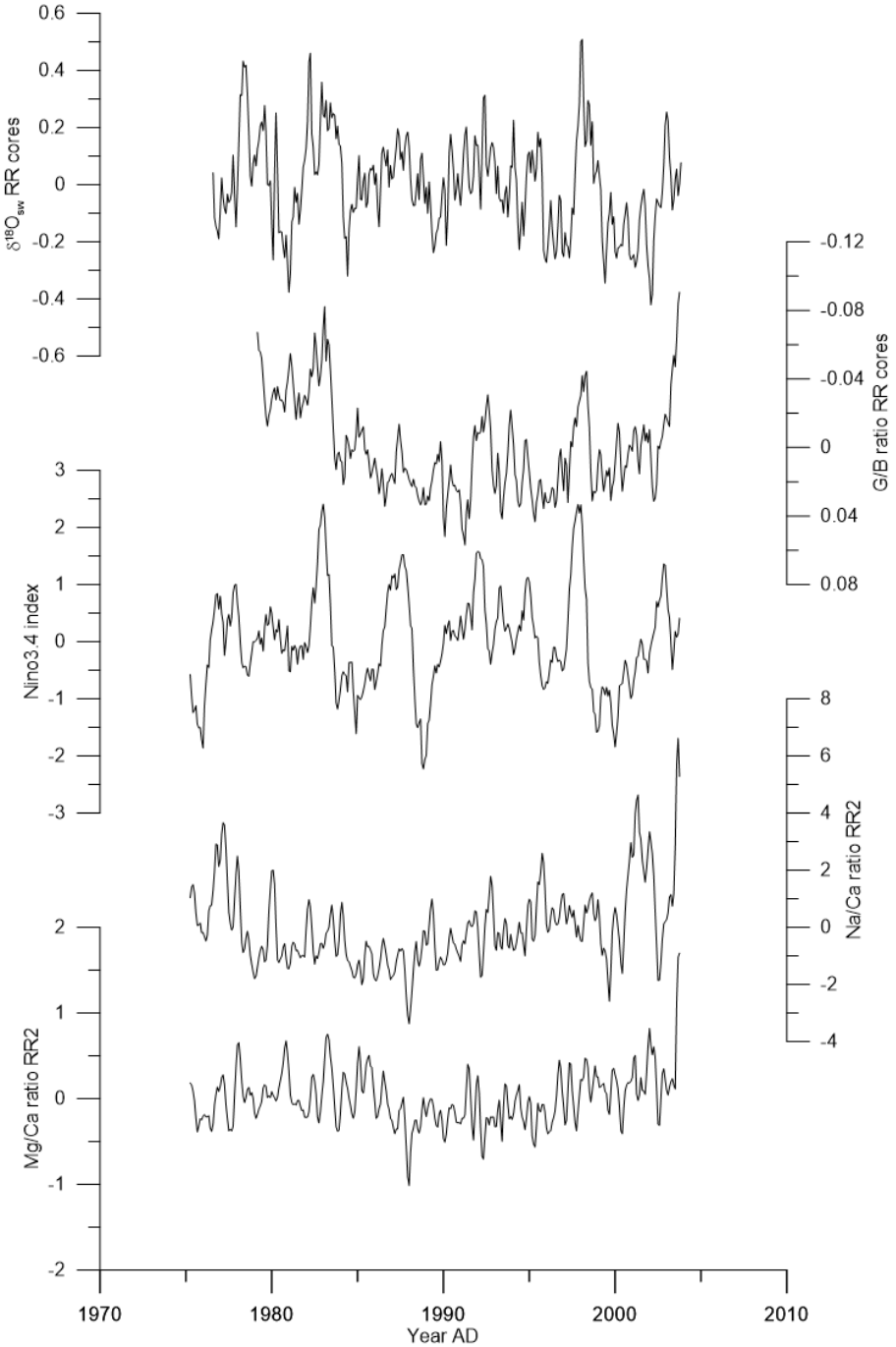

Figure 19. Linescan Laser Ablation ICP-MS data of Mg/Ca and Na/Ca ratios of the RR2 coral slab compared to $\delta^{18}O_{sw}$ reconstruction (RR2 and RR4 combined), the Nino3.4 index and G/B ratio of the RR coral slabs. Trace element data is smoothed and resampled to monthly data. To remove seasonal cycles, the anomalies of the data is displayed. Axes are chosen so that correlations of the different anomalies are in the same direction.

In Table 8, the anomalies of all measured trace elements are correlated with the anomalies of the climate indices, the anomalies of the SST and the anomalies of the G/B ratio and $\delta^{18}O_{sw}$ measurements. The graphs of these correlations are given in appendix. In Figure 20 the results of the correlations of Na/Ca, Mg/Ca, Al/Ca, and Sr/Ca anomalies with the Nino3.4 index anomalies are displayed in a 5 year running correlation. Figure 21 shows an overlaying graph of both Mg/Ca and Na/Ca ratio anomalies in respect to the anomalies of both the Nino3.4 index and the ITF index of Sebille et al. (2014).

Correlation (r)	Nino3.4	ITF	IOD	PDO	SST	G/B	$\delta^{18}O_{sw}$
Na/Ca	-0.035	-0.044	0.032	-0.090	0.003	-0.087	-0.173
Al/Ca	0.081	0.063	0.003	0.159	-0.240	0.007	0.035
Mg/Ca	-0.013	0.165	-0.057	-0.049	0.024	-0.141	-0.093
Sr/Ca	-0.041	0.107	0.090	0.106	-0.257	-0.043	-0.044
Ba/Ca	0.031	0.075	0.052	0.004	0.078	-0.156	-0.043

Table 8. Correlation between the measured trace elements in the RR2 coral slab with the most important climate indices affecting the Berau delta system and the G/B ratio and $\delta^{18}O_{sw}$. All data is displayed as anomalies to remove seasonal cycles. Correlations are constructed with the Climate Explorer database (KNMI; climexp.knmi.nl).Note: all correlations were computed assuming there was no lag in any of the $\delta^{18}O_{sw}$ data (lag=0). Graphs of these correlations are given in appendix.

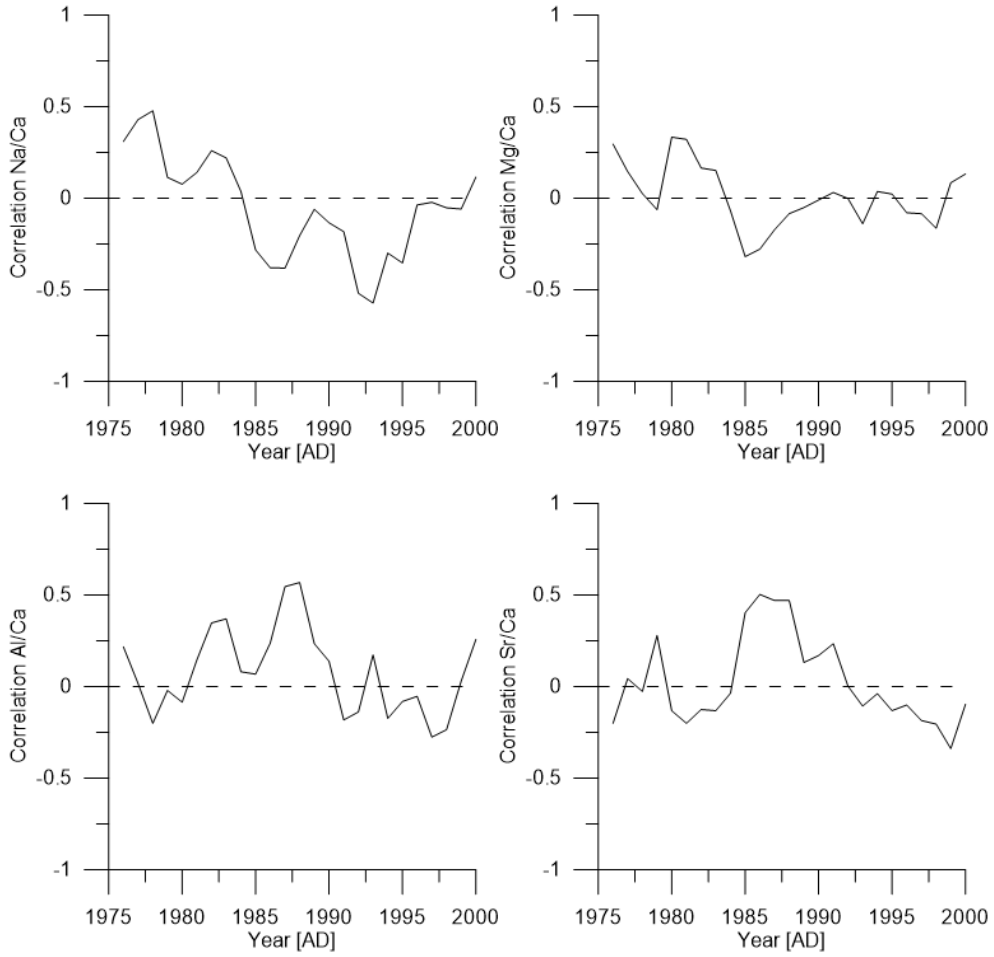

Figure 20. 5 year running correlation between the anomalies of the trace elements of Na/Ca, Mg/Ca, Al/Ca, and Sr/Ca with the Nino 3.4 index anomalies.

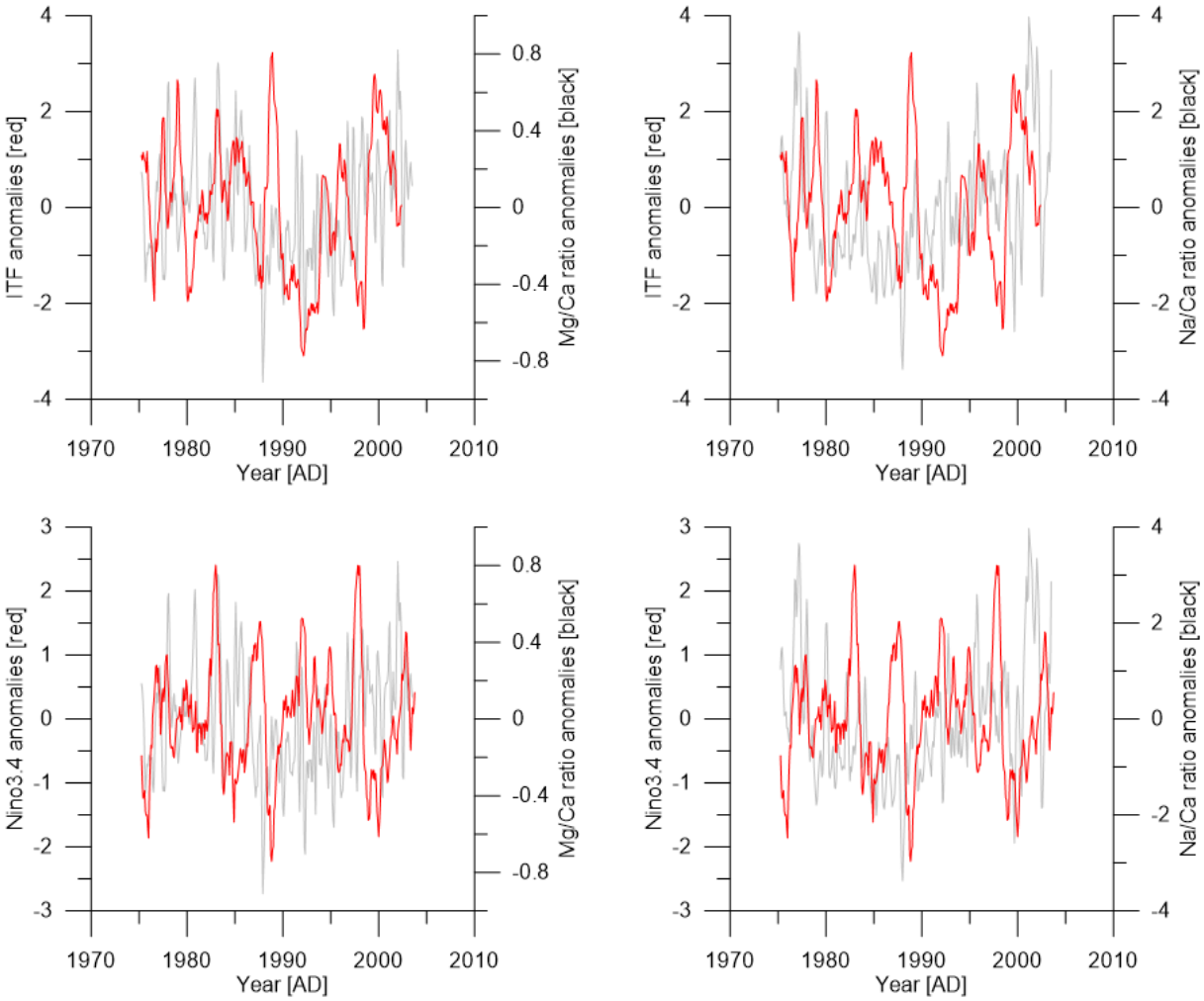

Figure 21. Overlapping graphs of both Mg/Ca (left) and Na/Ca (right) ratio anomalies with Nino3.4 (lower) and ITF (upper) anomalies. Both climate indices are displayed in red.

Table 8 shows that there is no significant correlation between any of the measured trace elements with the other measurement proxies and the climate indices. As already found in the raw data (Figure 15), the Sr/Ca, Al/Ca and Ba/Ca ratios do not show clear annual cycles and can therefore not be used as a proxy neither for a proper reconstruction of the Berau delta system. Although Na/Ca and Mg/Ca show clear annual cycles, there is no correlation found in the running correlation (Figure 20). Also in the overlapping graphs (Figure 21), no clear correlation is visible.

A possible reason for the absence of a good correlation between the more validated proxies of Mg/Ca and Sr/Ca as proxy for SST will possibly be the small variations in SST in the research area. The trace element Laser Ablation ICP-MS linescan data seems not to work as a proxy for the Berau delta system, most likely due to a to high error in the measurements. Limitations of the Laser Ablation linescan measurements are given in chapter *5.2.1.*

Sr/Ca ratios for other Berau delta system coral cores have been measured by Pascher (2012). Results of these datasets, combined with the Sr/Ca ratio measurements of the RR2 coral core of this research are shown in Figure 22. Instead of measuring trace elements with linescan Laser Ablation, the coral cores of Pascher (2012) have been measured with powder material in a HR-ICP-MS (Thermo Scientific ELEMENT-2), which is a more common method for coral trace element measurements.

The results of this research RR2 Sr/Ca ratio measurement have much larger fluctuations compared to the 3 measured Sr/Ca ratios by Pascher (2012) (Figure 22). The laser ablation linescan technique is not yet a commonly used method to measure trace elements on coral slabs [see *5.2.1 Limitations trace element proxies*]. More research is needed to obtain the best possible settings to measure these coral slabs. Although no correlation has been found in this research, the seasonal cycles in Mg/Ca and Na/Ca ratios show that the laser ablation technique on coral slabs can potentially give a good reconstruction of the climate variability in the area, and show that a high quality reconstruction can be achieved.

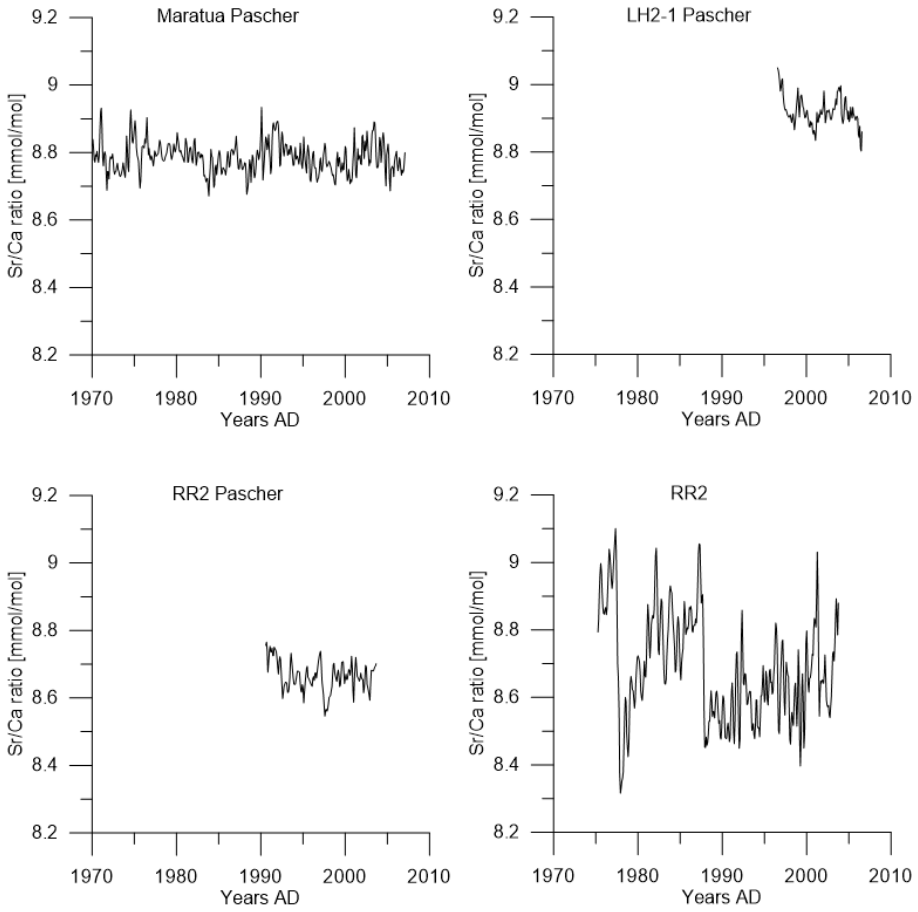

Figure 22. Sr/Ca ratio measurements of Pascher (RR2, LH2-1 and Maratua) and the RR2 measurements of this research.

5.2.1. Limitations trace element proxies

Measuring trace elements with laser ablation can give an extreme accurate representation of the coral slab as the amount of data points can be up to more than 1000 data points per millimetre. Still, the pores in the coral slabs can be up to more than a millimetre in diameter, which is much larger as the diameter of the laser spot. In order to gain significant results, the data needs to be smoothed. Whatever smoothing method is selected, in all cases valuable data is lost in the process. For this research the trace element data was smoothed by Matlab (Version 9.0, Mathworks). The method of smoothing of this research can still be improved by optimizing the settings of the Laser Ablation ICP-MS Linescan (e.g. decrease the amount of measured elements and construct a better standard for coral trace element measurements) and the settings of the Matlab smoothing settings (e.g. removing outliers and improving the Savitzky-Golay filtering).

Besides the smoothing of the obtained laser ablation data, also the settings of the measurements can still be optimized. For the method development of this research, only one coral slab was used. In order to increase the reliability of the laser ablation trace element measurements, more analysis is needed on more and different coral cores. This can also increase the knowledge about Na/Ca ratios as a possible proxy for salinity.

The correlation between the different climate variabilities studied for this research (El Niño-Southern Oscillation, Indian Ocean Dipole, Pacific Decadal Oscillation and the Indonesian Throughflow) is still highly unknown but is presumably there. Although a correlation has been found between the different conventional proxies and the El Niño-Southern Oscillation, PDO and the ITF, these correlations are not found with the different trace element proxies. The absence of a good correlations is probably caused by the low accuracy of the trace element measurements.

Although no good reconstruction of the Berau delta system was possible based on the measured coral trace elements, the laser ablation linescan technique show high potential as an alternative for the more common HR-ICP-MS (Thermo Scientific ELEMENT-2) measurements. The preparation and measuring of the laser ablation linescan is much less time consuming and has the potential to be much more accurate.

5.3. The Berau delta system

This study aims to reconstruct the climate variability of the Berau delta system over the last few decades. For this reconstruction, proxy datasets of $\delta^{18}O$, $\delta^{13}C$ and G/B ratios of different coral slabs were used. Besides that, also trace element measurements on one of the coral slabs was constructed in order to investigate a new proxy for salinity (i.e. Na/Ca ratio). Besides the Na/Ca measurements, also the trace elements of Sr/Ca, Mg/Ca, Ba/Ca and Al/Ca were measured for this coral slab. All different proxies were correlated with the different climate indices that are expected to influence the research area (ENSO, ITF, PDO and IOD). Results of a Morlet Wavelet Power Spectrum (Torrence and Compo, 1998) of the different proxies as well as the power spectrum of the Nino3.4 index, which was found to be the most important climate variability, are shown in Figure 23. The spectral analysis (AnalySeries, version 1.1.1, Paillard et al., 1996) of these proxies are displayed in Figure 24.

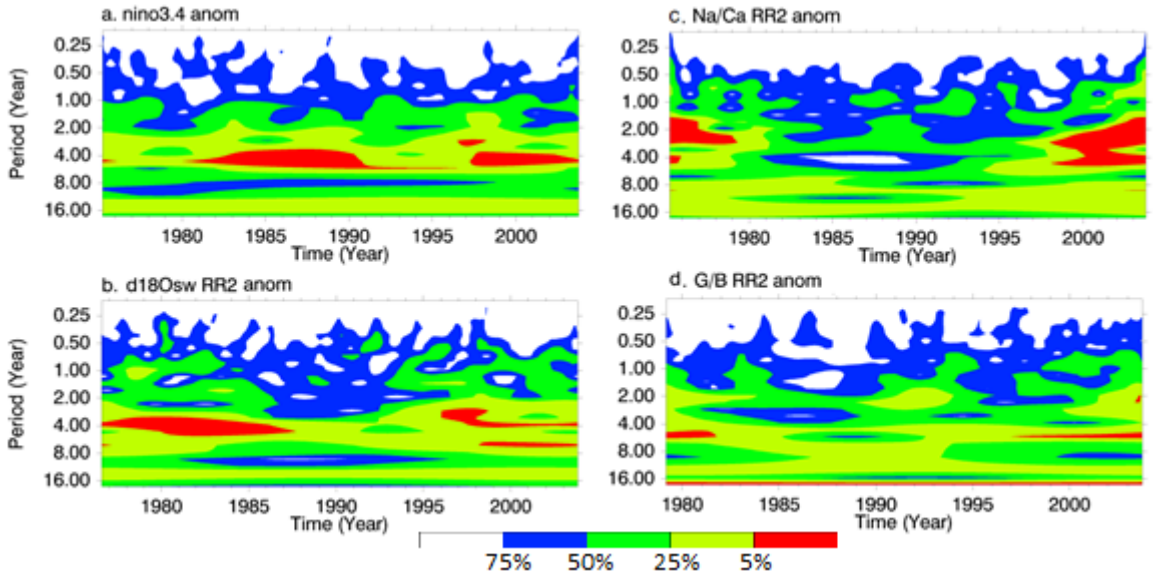

Figure 23. Morlet Wavelet Power Spectrum of a) Nino3.4 index anomalies, b) $\delta^{18}O_{sw}$ RR2 anomalies, c) Na/Ca ratio anomalies of core RR2 and d) G/B ratio anomalies of RR2. Contour levels display the percentage of the wavelet power that is above this level.

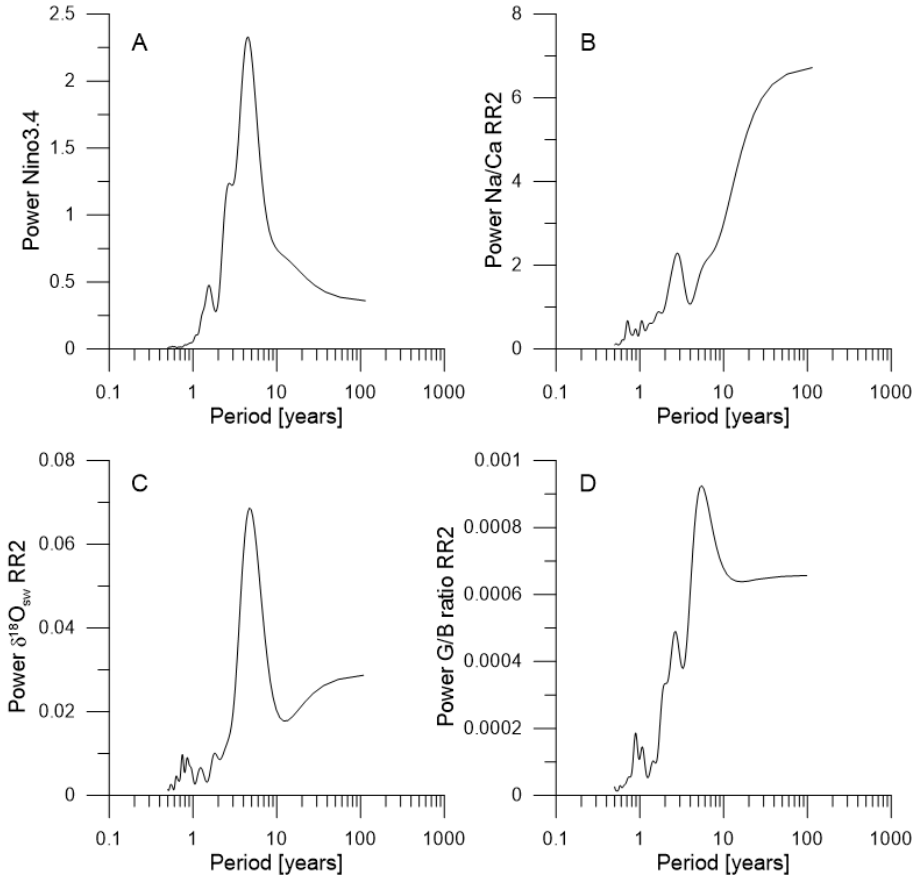

Figure 24. Spectral analysis, Blackman Tukey of a) Nino3.4 index anomalies, b) Na/Ca ratio anomalies of core RR2, c) $\delta^{18}O_{sw}$ RR2 anomalies, and d) G/B ratio anomalies of RR2.

The Power spectrum and spectral analysis show a peak in periodicity of the Nino3.4 index around 4.4 years. This periodicity is also found in the $\delta^{18}O_{sw}$ anomalies data of the RR2 coral cores (peak at 4.8 years), and to a less extend in the G/B anomalies data of the RR2 coral core (peak at 5.4 years). For the Na/Ca ratio anomalies of this core, no clear periodicity was found.

The results of the Laser Ablation ICP-MS linescan trace element ratios did not show a clear correlation with any of the climate indices and could therefore not be used for the reconstruction of the climate variability of the Berau delta system. On the other hand, the results of the G/B ratios, $\delta^{18}O$ and to a lesser extent $\delta^{13}C$ could be correlated with different climate indices to reconstruct the Berau delta system.

Clear seasonal cycles were found in all of the conventional proxies, as well as in trace element data of Na/Ca and Mg/Ca ratios. The amplitude of these cycles were stronger in the corals that are located closer to the shore. This indicates that the most important effect influencing the Berau delta system are fluvial processes (i.e. the Berau River) instead of marine processes (i.e. the Indonesian Throughflow). The impact of the Berau River was found in lesser extend for the coral cores that are located further offshore. For these cores the marine processes (i.e. the Indonesian Throughflow) were found to be important as well.

This conclusion is enhanced due to the correlations that are found between the different conventional proxies and the climate indices. The strongest impact of climate variability for all the coral cores (both close to shore and the more distant coral cores) was found to be the El Niño-Southern Oscillation. This oscillation is highly related to the precipitation in the Berau catchment area and thereby the runoff of the Berau River (Ropelewski & Halpert, 1987). To a lesser extent, also a correlation was found between the measured proxies and the Pacific Decadal Oscillation. Due to the high correlation between the PDO and the Nino index, it still is not possible to find the direct impact of the PDO on the Berau delta system. Peaks in PDO that could be correlated to the proxies were also found in the Nino3.4 data. No clear correlation was found with the Indian Ocean Dipole. It can be concluded that the climate variability in the Pacific Ocean is more important for the Berau delta system than the variability of the Indian Ocean.

Also a correlation was found between the Indonesian Throughflow and the measured proxies. This correlation was highest for the distant coral cores. Marine processes seems to be most important for the coral cores that are located further offshore.

The clear correlation of the ITF and PDO with the different measured anomalies was less clear as the correlation of the measurements with the Nino3.4 index. It is already known that the ITF and PDO are closely correlated to the Nino3.4 index (Tillinger and Gordon, 2009; van Sebille et al., 2014; Wang et al., 2014). This makes it difficult to find the effective impact of the climate variabilities on the Berau delta system.

6. Conclusion

Aim of this study was to reconstruct the climate variability of the Berau delta system over the last few decades, using coral sampled in a transect from the river mouth of the Berau River to the open ocean. The special objective of this study was to develop a method for the potential Na/Ca salinity proxy by using a Laser Ablation ICP-MS linescan technique. The results of this new technique, in combination with the other proxy datasets of $\delta^{18}O$, $\delta^{13}C$, Sr/Ca, Ba/Ca, Mg/Ca and G/B ratios, were correlated to each other and to different climate indices (Nino3.4, PDO, IOD and ITF) the find the most important factor influencing the Berau delta system.

The results of the trace elements of the Laser Ablation linescan did not show a clear correlation with any of the climate indices and were therefore not used in the reconstruction of the Berau delta system. Still, Na/Ca and Mg/Ca ratios show seasonal cycles corresponding to the expected peaks and lows of the river runoff of the Berau River and can be used as a potential proxy for sea surface salinity. The technique of linescan Laser Ablation has high potential in fast and easy measuring trace elements in coral, although it needs to be developed in order to reduce the error (i.e. large offset and high amplitude) in the data. It still is highly uncertain if Na/Ca ratio can be used as a proxy for salinity, although the seasonal cycles show a possible correlation between the two.

Based on the more conventional $\delta^{18}O$, $\delta^{13}C$ and G/B ratio proxies of the coral slabs, the most important factors influencing the Berau delta system have been reconstructed. All three proxies show the best correlation with the Nino3.4 index, especially the major El Niño events were clearly visible in the data. Besides the correlation with Nino3.4, also less clear correlations have been found with the Pacific Decadal Oscillation index and the Indonesian Throughflow. Correlations with the Indian Ocean Dipole were very weak.

In conclusion it seems the Berau delta system is mostly influenced by the El Niño-Southern Oscillation, which is highly related to the precipitation in the Berau catchment area. Due to the normal high precipitation in the research area, especially the dry events during an El Niño are clearly visible in the coral data. The best correlation of the Nino3.4 index was found with the $\delta^{18}O_{sw}$ data. This river runoff proxy has a better correlation in respect to the erosion proxy of G/B ratio as the El Niño-Southern Oscillation has more impact on precipitation compared to erosion in the catchment area of the Berau River. Erosion not only depend solely on the amount of precipitation as well as the intensity of the precipitation and the vegetation cover.

The effect of changes in river runoff are best visible in the coral cores that are located close to the shoreline. The coral cores that are located further offshore show less impact of the river runoff and are more influenced by the oceanic processes (i.e. Indonesian Throughflow). Due to the result of commercial logging of the mountainous rainforest in the catchment area of the Berau River, it is expected that the increase of river runoff and sediment fluxes will have a great influence on the formation of the coral in the Berau delta system, especially the corals that are located close to the shoreline.

References

Allemand, D., Ferrier-Pagès, C., Furla, P., Houlbrèque, F., Puverel, S., Reynaud, S., Tambutté, É., Tambutté, S., & Zoccola, D. (2004). Biomineralisation in reef-building corals: from molecular mechanisms to environmental control. *Comptes Rendus Palevol*, *3*(6), 453-467.

Ambarwulan, W. (2010, September). Remote Sensing of Tropical Coastal Waters: Study of the Berau Estuary, East Kalimantan, Indonesia. ITC.

Barker, S., Greaves, M., & Elderfield, H. (2003). A study of cleaning procedures used for foraminiferal Mg/Ca paleothermometry. *Geochemistry, Geophysics, Geosystems*, *4*(9).

Benway, H. M., & Mix, A. C. (2004). Oxygen isotopes, upper-ocean salinity, and precipitation sources in the eastern tropical Pacific. *Earth and Planetary Science Letters*, *224*(3), 493-507.

Bindoff, N.L., P.A. Stott, K.M. AchutaRao, M.R. Allen, N. Gillett, D. Gutzler, K. Hansingo, G. Hegerl, Y. Hu, S. Jain, I.I. Mokhov, J. Overland, J. Perlwitz, R. Sebbari and X. Zhang, 2013: Detection and Attribution of Climate Change: from Global to Regional. In: Climate Change 2013: The Physical Science Basis. Contribution of Working Group I to the Fifth Assessment Report of the Intergovernmental Panel on Climate Change [Stocker, T.F., D. Qin, G.-K. Plattner, M. Tignor, S.K. Allen, J. Boschung, A. Nauels, Y. Xia, V. Bex and P.M. Midgley (eds.)]. Cambridge University Press, Cambridge, United Kingdom and New York, NY, USA.

Buerger, P., Schmidt, G. M., Wall, M., Held, C., & Richter, C. (2015). Temperature tolerance of the coral Porites lutea exposed to simulated large amplitude internal waves (LAIW). *Journal of Experimental Marine Biology and Ecology*, *471*, 232-239.

Buschman, F. A., Hoitink, A. J. F., Van Der Vegt, M., & Hoekstra, P. (2009). Subtidal water level variation controlled by river flow and tides. *Water resources research*, *45*(10).

Buschman, F. A., Hoitink, A. J. F., de Jong, S. M., Hoekstra, P., Hidayat, H., & Sassi, M. G. (2012). Suspended sediment load in the tidal zone of an Indonesian river. *Hydrology and Earth System Sciences*, *16*(11), 4191-4204.

Cahyarini, S. Y., Pfeiffer, M., Timm, O., Dullo, W. C., & Schönberg, D. G. (2008). Reconstructing seawater δ 18 O from paired coral δ 18 O and Sr/Ca ratios: Methods, error analysis and problems, with examples from Tahiti (French Polynesia) and Timor (Indonesia). *Geochimica et Cosmochimica Acta*, *72*(12), 2841-2853.

Christensen, J.H., K. Krishna Kumar, E. Aldrian, S.-I. An, I.F.A. Cavalcanti, M. de Castro, W. Dong, P. Goswami, A. Hall, J.K. Kanyanga, A. Kitoh, J. Kossin, N.-C. Lau, J. Renwick, D.B. Stephenson, S.-P. Xie and T. Zhou, 2013: Climate Phenomena and their Relevance for Future Regional Climate Change. In: Climate Change 2013: The Physical Science Basis. Contribution of Working Group I to the Fifth Assessment Report of the Intergovernmental Panel on Climate Change [Stocker, T.F., D. Qin, G.-K. Plattner, M. Tignor, S.K. Allen, J. Boschung, A. Nauels, Y. Xia, V. Bex and P.M. Midgley (eds.)]. Cambridge University Press, Cambridge, United Kingdom and New York, NY, USA.

Corrège, T. (2006). Sea surface temperature and salinity reconstruction from coral geochemical tracers. *Palaeogeography, Palaeoclimatology, Palaeoecology*, *232*(2), 408-428.

Fairbanks, R. G., Evans, M. N., Rubenstone, J. L., Mortlock, R. A., Broad, K., Moore, M. D., & Charles, C. D. (1997). Evaluating climate indices and their geochemical proxies measured in corals. *Coral Reefs*, *16*(1), S93-S100.

Fallon, S. J., McCulloch, M. T., van Woesik, R., & Sinclair, D. J. (1999). Corals at their latitudinal limits: laser ablation trace element systematics in Porites from Shirigai Bay, Japan. *Earth and Planetary Science Letters*, *172*(3), 221-238.

Felis, T., Pätzold, J., Loya, Y., & Wefer, G. (1998). Vertical water mass mixing and plankton blooms recorded in skeletal stable carbon isotopes of a Red Sea coral. *Journal of Geophysical Research-all series-*, *103*, 30-731.

Ferguson, J. E., Henderson, G. M., Kucera, M., & Rickaby, R. E. M. (2008). Systematic change of foraminiferal Mg/Ca ratios across a strong salinity gradient. *Earth and Planetary Science Letters*, *265*(1), 153-166.

Glantz, M. H. (2001). *Currents of change: impacts of El Niño and La Niña on climate and society*. Cambridge University Press.

Gordon, A.L., Susanto, R. D., & Vranes, K. (2003). Cool Indonesian throughflow as a consequence of restricted surface layer flow. *Nature, 425*(6960), 824-828.

Grove, C. A., Nagtegaal, R., Zinke, J., Scheufen, T., Koster, B., Kasper, S., McCulloch, M.T., van den Bergh, G. and Brummer, G. J. A. (2010). River runoff reconstructions from novel spectral luminescence scanning of massive coral skeletons. *Coral Reefs*, *29*(3), 579-591.

Grove, C. A. (2012). Madagascar s climate history unlocked by giant corals. Doctoral theses, Vrije Universiteit Amsterdam.

Grove, C. A., Zinke, J., Peeters, F., Park, W., Scheufen, T., Kasper, S., Randriamanantsoa, B., McCulloch, M.T. and Brummer, G. J. (2013). Madagascar corals reveal a multidecadal signature of rainfall and river runoff since 1708. *Climate of the Past*, *9*(2), 641-656.

Grove, C. A., Rodriguez-Ramirez, A., Merschel, G., Tjallingii, R., Zinke, J., Macia, A., & Brummer, G. J. A. (2015). UV-Spectral Luminescence Scanning: Technical Updates and Calibration Developments. In *Micro-XRF Studies of Sediment Cores* (pp. 563-581). Springer Netherlands.

Hathorne, E. C., Gagnon, A., Felis, T., Adkins, J., Asami, R., Boer, W., Caillon, N., Case, D., Cobb, K.M., Douville, E., deMenocal., P., Eisenhauer, A., Garbe-Schönberg., D., Geibert, W., Goldstein, S., Hughen, K., Inoue, M., Kawahata, H., Kölling, M., Cornec, F.L., Linsley, B.K., McGregor, H.V., Montagna, P., Nurhati, I.S., Quinn, T.M., Raddatz, J., Rebaubier, H., Robinson, L., Sadekov, A., Sherrell, R., Sinclair, D., Tudhope, A.W., Wei, G., Wong, H., Wu, H.C., & You, C.F., (2013). Interlaboratory study for coral Sr/Ca and other element/Ca ratio measurements. *Geochemistry, Geophysics, Geosystems*,*14*(9), 3730-3750.

Henderson, G. M. (2002). New oceanic proxies for paleoclimate. *Earth and Planetary Science Letters*, *203*(1), 1-13.

Huang, B., Banzon, V. F., Freeman, E., Lawrimore, J., Liu, W., Peterson, T. C., Smith, T.M., Thorne, P.W., Woodruff, S.D., & Zhang, H. M. (2015). Extended reconstructed sea surface temperature version 4 (ERSST. v4). Part I: upgrades and intercomparisons. *Journal of Climate*, *28*(3), 911-930.

KNAW (2016, May 19), *From River to barrier Reef, the Berau system Retrieved*. Retrieved from https://www.knaw.nl/shared/resources/internationaal/indonesia/the_berau_system.pdf

KNMI Climate Exporer. (2016). Monthly Nino3.4 index. http://climxep.knmi.nl

Liu, Q. Y., Feng, M., Wang, D., & Wijffels, S. (2015). Interannual variability of the Indonesian Throughflow transport: A revisit based on 30 year expendable bathythermograph data. *Journal of Geophysical Research: Oceans*.

Mantua, N. J., Hare, S. R., Zhang, Y., Wallace, J. M., & Francis, R. C. (1997). A Pacific interdecadal climate oscillation with impacts on salmon production.*Bulletin of the american Meteorological Society*, *78*(6), 1069-1079.

Mantua, N. J., & Hare, S. R. (2002). The Pacific decadal oscillation. *Journal of oceanography*, *58*(1), 35-4

Marshall, J. F., & McCulloch, M. T. (2002). An assessment of the Sr/Ca ratio in shallow water hermatypic corals as a proxy for sea surface temperature.*Geochimica et Cosmochimica Acta*, *66*(18), 3263-3280.

McCulloch, M., Fallon, S., Wyndham, T., Hendy, E., Lough, J., & Barnes, D. (2003). Coral record of increased sediment flux to the inner Great Barrier Reef since European settlement. *Nature*, *421*(6924), 727-730.

Meyers, G. (1996). Variation of Indonesian throughflow and the El Niño-Southern Oscillation. *Journal of Geophysical Research: Oceans*, *101*(C5), 12255-12263.

Mitsuguchi, T., Matsumoto, E., Abe, O., Uchida, T., & Isdale, P. J. (1996). Mg/Ca thermometry in coral skeletons. *Science*, *274*(5289), 961-963.

Mitsuguchi, T., Matsumoto, E., & Uchida, T. (2003). Mg/Ca and Sr/Ca ratios of Porites coral skeleton: Evaluation of the effect of skeletal growth rate. *Coral Reefs*, *22*(4), 381-388.

Mitsuguchi, T., Uchida, T., & Matsumoto, E. (2010). Na/Ca variability in coral skeletons. *Geochemical Journal*, *44*(4), 261-273.

Moreau, M., Corrège, T., Dassié, E. P., & Le Cornec, F. (2015). Evidence for the non-influence of salinity variability on the Porites coral Sr/Ca palaeothermometer. *Climate of the Past*, *11*(3), 523-532.

Morgan, R. P. C. (2009). *Soil erosion and conservation*. John Wiley & Sons.

Nagtegaal, R., van den Bergh, G., Pascher, K., Jochum, K. P., & Brummer, G. A. (2011). Reconstructing inter annual Indonesian river discharge by high-resolution LA-ICPMS geochemistry and UV-luminescence scanning of corals. In *AGU Fall Meeting Abstracts* (Vol. 1, p. 0914).

Null, J. (2016, April 13), *El Niño and La Niña Years and Intensities.* Retrieved from ggweather.com/enso/oni.htm

Paillard, D., Labeyrie, L., & Yiou, P. (1996). Macintosh program performs time-series analysis. *Eos, Transactions American Geophysical Union*, *77*(39), 379-379.

Palmer, T. N., & Mansfield, D. A. (1984). Response of two atmospheric general circulation models to sea-surface temperature anomalies in the tropical east and west Pacific.

Paris, C. B., Helgers, J., Van Sebille, E., & Srinivasan, A. (2013). Connectivity Modeling System: A probabilistic modeling tool for the multi-scale tracking of biotic and abiotic variability in the ocean. *Environmental Modelling & Software*, *42*, 47-54.

Pascher, K. (2012) Using high-resolution geochemistry and luminescence signals in corals to investigate climate variability and sediment supply to the Berau delta/barrier reef system, East Kalimantan, Indonesia, *MSc thesis, Eberhard-Karls Universität Tübingen*.

Ramos, A. A., Inoue, Y., & Ohde, S. (2004). Metal contents in Porites corals: Anthropogenic input of river run-off into a coral reef from an urbanized area, Okinawa. *Marine Pollution Bulletin*, *48*(3), 281-294.

Ren, L., Linsley, B. K., Wellington, G. M., Schrag, D. P., & Hoegh-Guldberg, O. (2003). Deconvolving the δ 18 O seawater component from subseasonal coral δ 18 O and Sr/Ca at Rarotonga in the southwestern subtropical Pacific for the period 1726 to 1997. *Geochimica et Cosmochimica Acta*, *67*(9), 1609-1621.

Renema, W. (2006). Habitat variables determining the occurrence of large benthic foraminifera in the Berau area (East Kalimantan, Indonesia). *Coral Reefs*, *25*(3), 351-359.

Rhein, M., S.R. Rintoul, S. Aoki, E. Campos, D. Chambers, R.A. Feely, S. Gulev, G.C. Johnson, S.A. Josey, A. Kostianoy, C. Mauritzen, D. Roemmich, L.D. Talley and F. Wang, 2013: Observations: Ocean. In: Climate Change 2013: The Physical Science Basis. Contribution of Working Group I to the Fifth Assessment Report of the Intergovernmental Panel on Climate Change [Stocker, T.F., D. Qin, G.-K. Plattner, M. Tignor, S.K. Allen, J. Boschung, A. Nauels, Y. Xia, V. Bex and P.M. Midgley (eds.)]. Cambridge University Press, Cambridge, United Kingdom and New York, NY, USA.

Rodriguez-Ramirez, A., Grove, C. A., Zinke, J., Pandolfi, J. M., & Zhao, J. X. (2014). Coral luminescence identifies the Pacific Decadal Oscillation as a primary driver of river runoff variability impacting the southern Great Barrier Reef. *PloS one*, *9*(1).

Rohling, E. J. (2000). Paleosalinity: confidence limits and future applications. *Marine Geology*, *163*(1), 1-11.

Ropelewski, C. F., & Halpert, M. S. (1987). Global and regional scale precipitation patterns associated with the El Niño/Southern Oscillation. *Monthly weather review*, *115*(8), 1606-1626.

Saji, N. H., Goswami, B. N., Vinayachandran, P. N., & Yamagata, T. (1999). A dipole mode in the tropical Indian Ocean. *Nature*, *401*(6751), 360-363.

Sebille, E., Sprintall, J., Schwarzkopf, F. U., Sen Gupta, A., Santoso, A., England, M. H., Biastoch, A., and Böning, C. W. (2014). Pacific-to-Indian Ocean connectivity: Tasman leakage, Indonesian Throughflow, and the role of ENSO. *Journal of Geophysical Research: Oceans*, *119*(2), 1365-1382.

Sinclair, D. J., & McCulloch, M. T. (2004). Corals record low mobile barium concentrations in the Burdekin River during the 1974 flood: evidence for limited Ba supply to rivers?. *Palaeogeography, Palaeoclimatology, Palaeoecology*, *214*(1), 155-174.

Suzuki, A., Hibino, K., Iwase, A. and Kawahata, H. (2005). Intercolony variability of skeletal oxygen and carbon isotope signatures of cultured *Porites* corals: Temperature-controlled experiments. Geochimica et Cosmochimica Acta. Vol. 69, No. 18, pp. 4453-4462.

Swart, P. K., Leder, J. J., Szmant, A. M., & Dodge, R. E. (1996). The origin of variations in the isotopic record of scleractinian corals: II. Carbon. *Geochimica et Cosmochimica Acta*, *60*(15), 2871-2885.

Tarya, A., van der Vegt, M., & Hoitink, A. J. F. (2015). Wind forcing controls on river plume spreading on a tropical continental shelf. *Journal of Geophysical Research: Oceans*, *120*(1), 16-35.

Tarya, A., Hoitink, A.J.F., Van der Vegt, M., van Katwijk, M.M., & Hoeksema, B.W. (in preparation). Exposure of coastal ecosystem to river plume spreading in a tropical continental shelf.

Tillinger, D., & Gordon, A. L. (2009). Fifty Years of the Indonesian Throughflow*. *Journal of Climate*, *22*(23), 6342-6355.

Torrence, C., & Compo, G. P. (1998). A practical guide to wavelet analysis.*Bulletin of the American Meteorological society*, *79*(1), 61-78.

Trenberth, K.E., P.D. Jones, P. Ambenje, R. Bojariu, D. Easterling, A. Klein Tank, D. Parker, F. Rahimzadeh, J.A. Renwick, M. Rusticucci, B. Soden and P. Zhai, 2007: Observations: Surface and Atmospheric Climate Change. In: *Climate Change 2007: The Physical Science Basis*. Contribution of Working Group I to the Fourth Assessment Report of the Intergovernmental Panel on Climate Change [Solomon, S., D. Qin, M. Manning, Z. Chen, M. Marquis, K.B. Averyt, M. Tignor and H.L. Miller (eds.)]. Cambridge University Press, Cambridge, United Kingdom and New York, NY, USA.

de Villiers, S., Nelson, B. K., & Chivas, A. R. (1995). Biological controls on coral Sr/Ca and δ18O reconstructions of sea surface temperatures. *Science*,*269*(5228), 1247-1249.

Wang, B. S., Goodkin, N. F., Angeline, N., Switzer, A. D., You, C. F., & Hughen, K. (2011). Temporal distributions of anthropogenic Al, Zn and Pb in Hong Kong Porites coral during the last two centuries. *Marine pollution bulletin*,*63*(5), 508-515.

Wang, S., Huang, J., He, Y., & Guan, Y. (2014). Combined effects of the Pacific decadal oscillation and El Nino-southern oscillation on global land dry–wet changes. *Scientific reports*, *4*.

Watanabe, T., Winter, A., Oba, T., Anzai, R., & Ishioroshi, H. (2002). Evaluation of the fidelity of isotope records as an environmental proxy in the coral Montastraea. *Coral Reefs*, *21*(2), 169-178.

Wit, J. C., de Nooijer, L. J., Wolthers, M., & Reichart, G. J. (2013). A novel salinity proxy based on Na incorporation into foraminiferal calcite. *Biogeosciences*, *10*, 6375-6387.

Wyrtki, K. (1987). Indonesian throughflow and the associated pressure gradient. *Journal of Geophysical Research*, *92*(12), 941-12.

Zinke, J., Pfeiffer, M., Timm, O., Dullo, W. C., & Davies, G. R. (2005). Atmosphere–ocean dynamics in the Western Indian Ocean recorded in corals. *Philosophical Transactions of the Royal Society of London A: Mathematical, Physical and Engineering Sciences*, *363*(1826), 121-142.

Acknowledgement

I would like to thank everyone at the CSO department of the NIOZ, Texel and all the fellow students at the Potvis campus, Texel for the great time on the island. I enjoyed the great working atmosphere in the department.

I would like to thank my supervisors, Prof. Gert-Jan Reichart and Dr. Rick Hennekam for the outstanding supervision and their advice and feedback during the entire process, Wim Boer for helping with the process of developing a method for measuring the trace elements, and Piet van Geaver for his help with the measurements of the stable isotope measurements.

Appendix

Na anomalies of the RR2 coral core correlated with the different climate indices and the measured conventional proxies. All data was resampled to a monthly dataset. The correlation data is given in table 8.

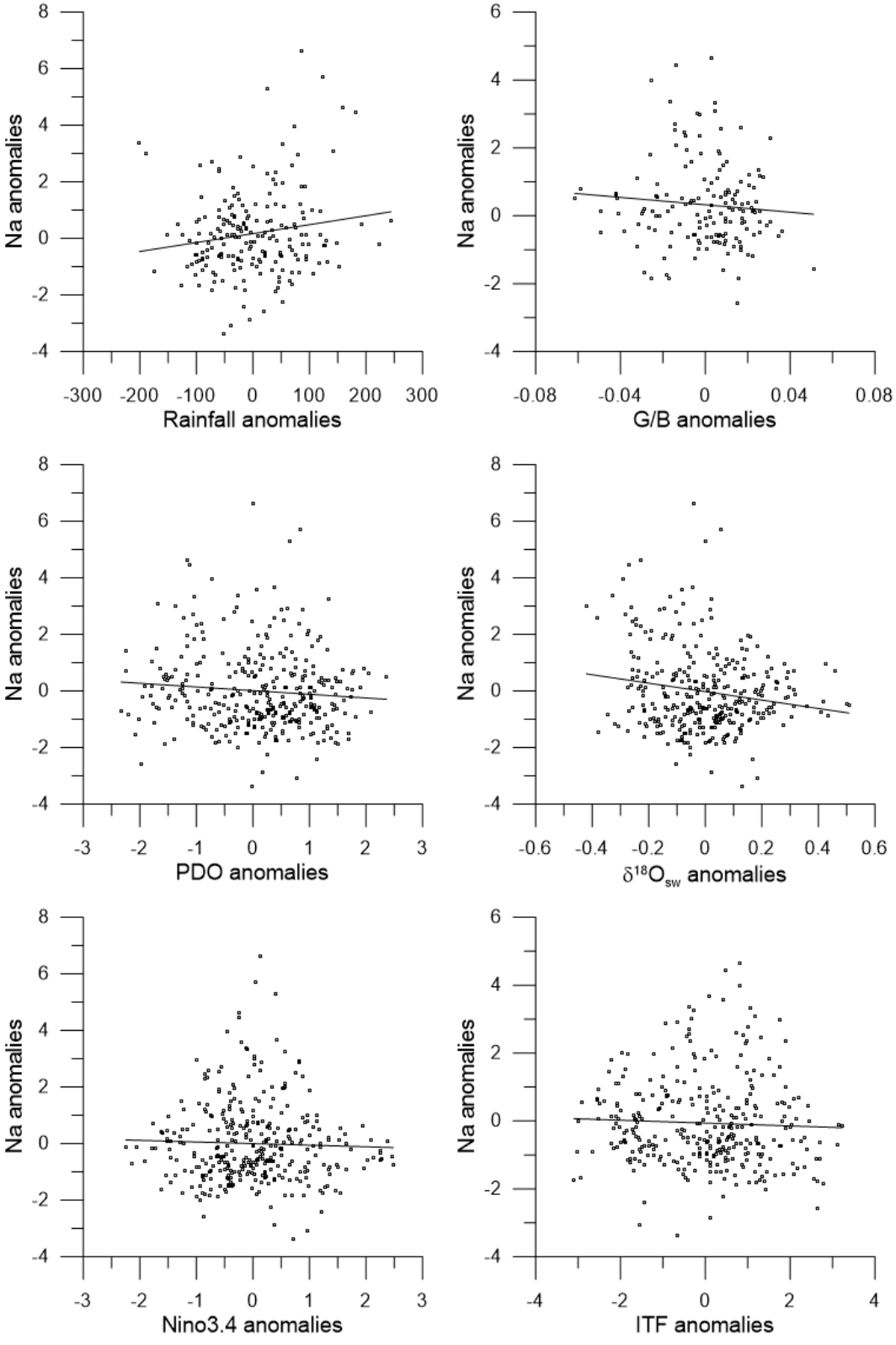

Al anomalies of the RR2 coral core correlated with the different climate indices and the measured conventional proxies. All data was resampled to a monthly dataset. The correlation data is given in table 8.

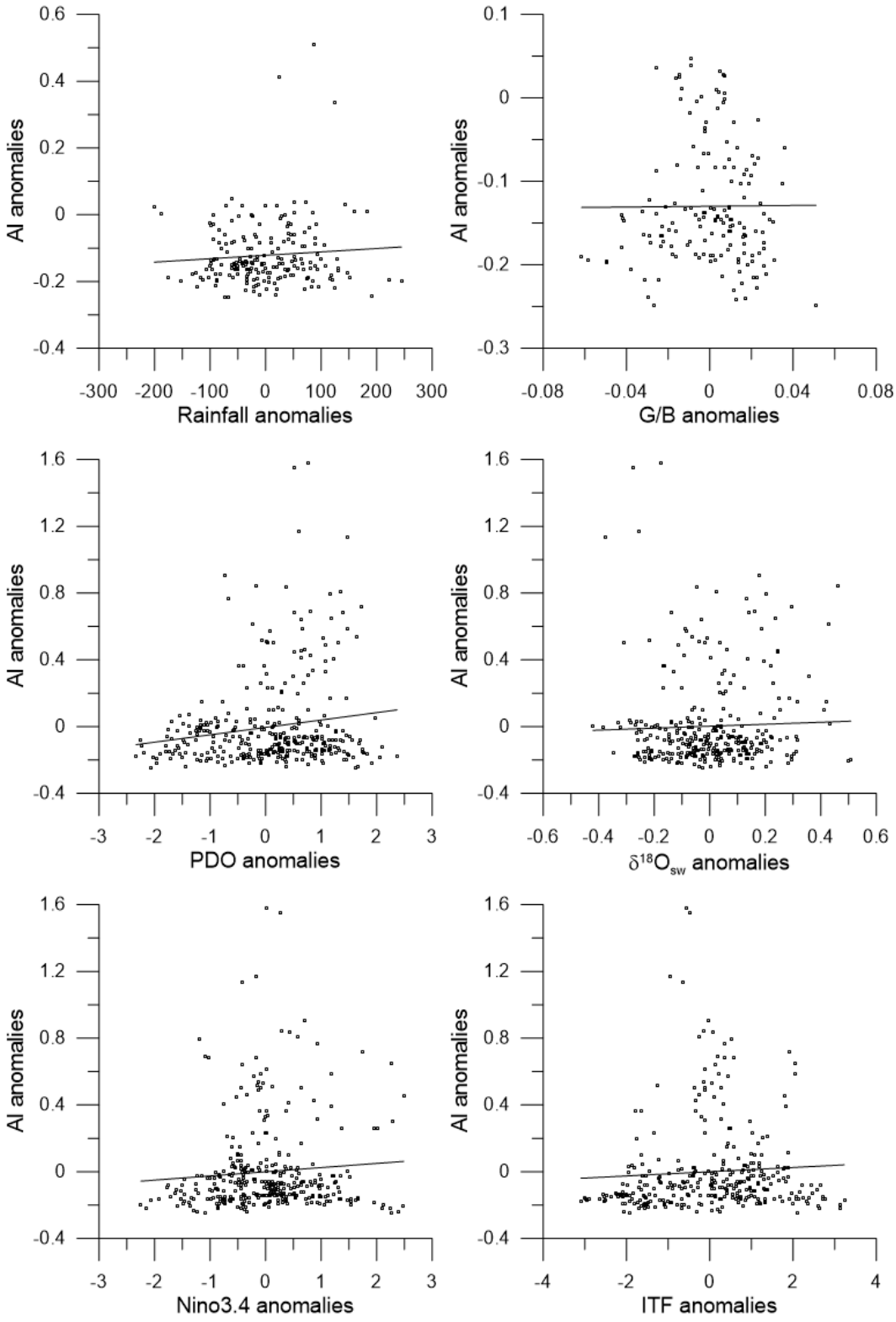

Mg anomalies of the RR2 coral core correlated with the different climate indices and the measured conventional proxies. All data was resampled to a monthly dataset. The correlation data is given in table 8.

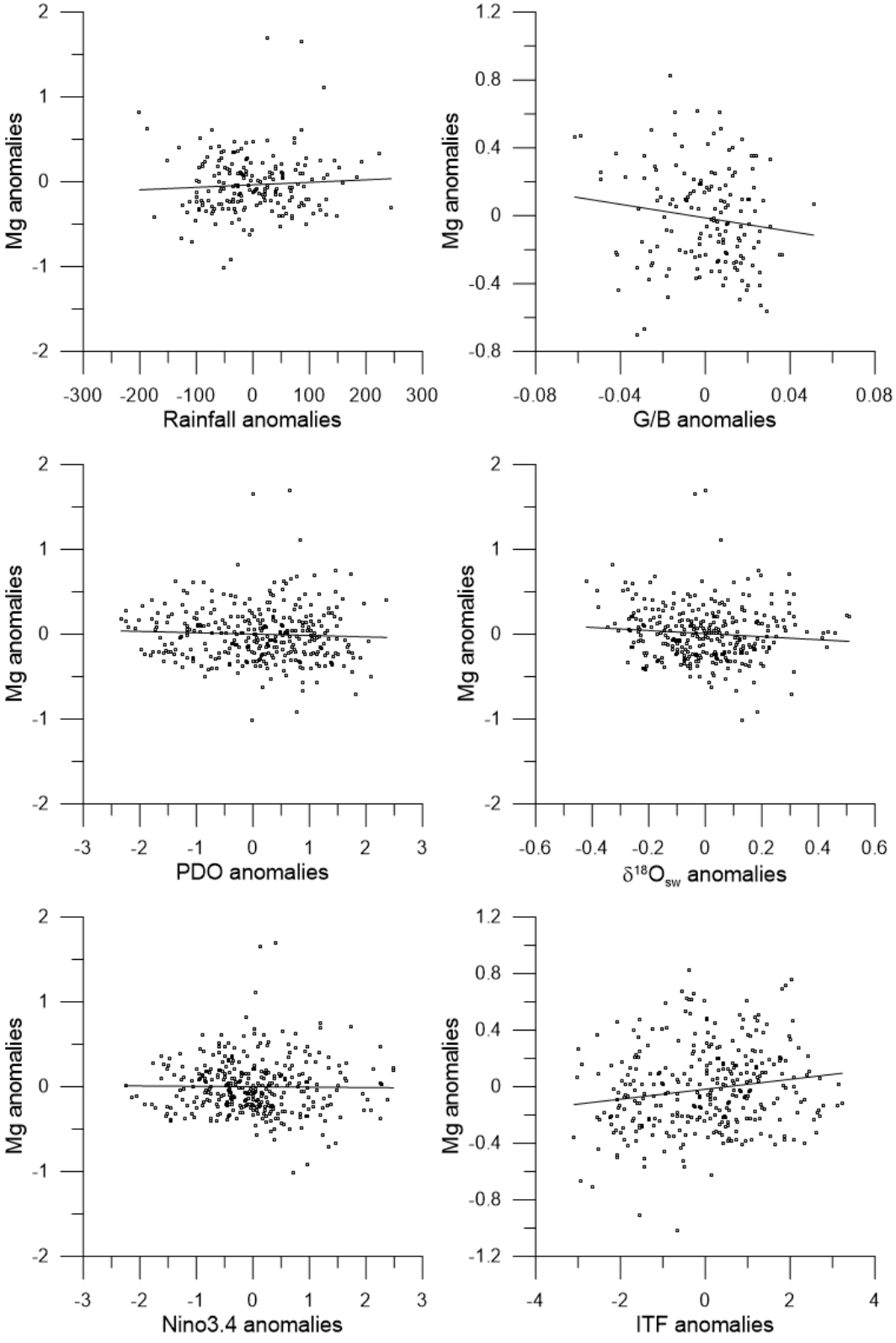

Sr anomalies of the RR2 coral core correlated with the different climate indices and the measured conventional proxies. All data was resampled to a monthly dataset. The correlation data is given in table 8.